AMANDA ÁVILA CARDOSO

HYDRAULIC AND CHEMICAL MECHANISMS CONTROLLING STOMATAL AND XYLEM RESPONSES TO CHANGES IN VAPOR PRESSURE DEFICIT

Thesis submitted to the Plant Physiology Graduate Program of the Universidade Federal de Viçosa in partial fulfillment of the requirements for the degree of Doctor Scientiae.

VIÇOSA
MINAS GERAIS – BRASIL
2017

Ficha catalográfica preparada pela Biblioteca Central da Universidade Federal de Viçosa - Câmpus Viçosa

T
C268h
2017

Cardoso, Amanda Ávila, 1990-
Hydraulic and chemical mechanisms controlling stomatal and xylem responses to changes in vapor pressure deficit / Amanda Ávila Cardoso. – Viçosa, MG, 2017.
v, 71f. : il. (algumas color.) ; 29 cm.

Orientador: Fábio Murilo da Matta.
Tese (doutorado) - Universidade Federal de Viçosa.
Inclui bibliografia.

1. Fisiologia vegetal. 2. Hormônios vegetais. 3. Plantas - Relações hídricas. I. Universidade Federal de Viçosa. Departamento de Biologia Vegetal. Programa de Pós-graduação em Fisiologia Vegetal. II. Título.

CDD 22 ed. 571.2

AMANDA ÁVILA CARDOSO

HYDRAULIC AND CHEMICAL MECHANISMS CONTROLLING STOMATAL AND XYLEM RESPONSES TO CHANGES IN VAPOR PRESSURE DEFICIT

Thesis submitted to the Plant Physiology Graduate Program of the Universidade Federal de Viçosa in partial fulfillment of the requirements for the degree of *Doctor Scientiae*.

APPROVED: November 17th, 2017.

Leandro Elias Morais

Franklin Magnum de Oliveira Silva

Samuel Cordeiro Vitor Martins
(Co-Adviser)

Agustin Zsögön

Fábio Murilo da Matta
(Adviser)

ACKNOWLEDGEMENTS

I am grateful to Universidade Federal de Viçosa and University of Tasmania for having me as student, to professors from the Plant Physiology Graduate Program for rendering me so much knowledge, and to CNPq and FAPEMIG for financial support.

My deepest gratitude is extended to Fábio DaMatta (adviser) and Samuel Martins (co-adviser). Your mentorship and support during my entire candidature were essential for this thesis to come true. I also acknowledge your friendship, for plenty of happy and funny moments, and for allowance to pursue a ten-month research period in Tasmania, which rendered me a highly rewarding and important opportunity to develop as a research scientist. Especially to Samuel, thank you for holding my hand in my first steps at DaMatta's laboratory. Thank you for teaching me so much about leaf gas exchange and plant hydraulics, instilling me a great and ongoing passion for the subject.

My even deep gratitude goes to my Australian supervisors Tim Brodribb and Scott McAdam. I am so lucky to have spent time working with this couple. Your profound knowledge of and passion for plants is really inspiring. I will always miss working with you two.

I am also grateful to a number of people who have provided support to and assisted with my research projects in both Brazil and Australia, i.e. Rodrigo Ávila, Junior Molina, Kleiton Machado, Wellington Almeida, Marcela Barbosa, Dinorah Moraes, Marco Juárez, Feng-Ping Zhang, Greg Jordan, Luis Villalobos, Madeline Murphy, Christopher Lucani, Ross Deans, Marc Carriquí, Shelley Urquhart and Theodore Dimitriou.

I thank my close friends, specially Luana Pereira and Kelly Spencer, and my family that have always supported me. To my family, thank you for inspiring me to dream so high, and for believing that I could be better. And to Cris, thank you for your affection, huge support and endless patience. You are the one when things get hard. Thank you for that.

I thank you God for caring me through all storms when I needed you the most.

TABLE OF CONTENTS

RESUMO

CARDOSO, Amanda Ávila, D.Sc., Universidade Federal de Viçosa, novembro de 2017. **Hydraulic and chemical mechanisms controlling stomatal and xylem responses to changes in vapor pressure deficit.** Orientador: Fábio Murilo da Matta. Coorientador: Samuel Cordeiro Vitor Martins.

Estômatos são pequenos poros, localizados na epiderme foliar de quase todas as plantas vasculares, responsáveis pelas trocas gasosas entre a atmosfera e o interior foliar. O poro estomático é delimitado por células-guarda, que aumentam e diminuem em volume em resposta a estímulos endógenos e externos. Em particular, as flutuações no déficit de pressão de vapor entre a folha e a atmosfera (DPV) ditam a abertura estomática ao longo do dia, com influências nas trocas gasosas e na hidratação foliar. Neste estudo, foi testado em girassol (Helianthus annuus) e em soja (Glycine max) se o ácido abscísico (ABA) é importante na regulação das respostas estomáticas ao DPV em plantas ajustadas osmoticamente, ou se a influência do potencial hídrico foliar (Ψ_l) sobre a resposta estomática supera a influência desse hormônio. Também foi examinada a capacidade de folhas de girassol de se aclimatarem a uma reduzida disponibilidade hídrica, modificando a sensibilidade do estômato e do xilema ao déficit de água no solo. A condutância estomática durante as transições de DPV não foram associadas ao Ψ_l, mas tanto o fechamento estomático em alto DPV quanto a abertura estomática no retorno ao baixo DPV foram fortemente influenciadas pela concentração de ABA na folha. Demonstrou-se que a produção de ABA foliar em alto DPV é desencadeada por variações na turgescência celular e não por alterações no Ψ_l per se. Plantas de girassol ajustadas osmoticamente mantiveram maior abertura estomática a Ψ_l mais negativos e uma reduzida sensibilidade de dano fotossintético ao estresse hídrico. Ao mesmo tempo, a vulnerabilidade hidráulica do xilema variou em resposta à condição de crescimento, com plantas sob seca produzindo condutos xilemáticos com paredes celulares mais grossas e mais resistentes à cavitação. A plasticidade coordenada entre o potencial osmótico e a vulnerabilidade do xilema permite que girassóis crescidos em seca extraiam água do solo com mais segurança, protegendo o xilema das folhas do embolismo. A alta plasticidade da vulnerabilidade do xilema encontrada em girassol pode sugerir uma estratégia alternativa em espécies herbáceas durante o déficit hídrico.

ABSTRACT

CARDOSO, Amanda Ávila, D.Sc., Universidade Federal de Viçosa, November, 2017. **Hydraulic and chemical mechanisms controlling stomatal and xylem responses to changes in vapor pressure deficit.** Adviser: Fábio Murilo da Matta. Co-Adviser: Samuel Cordeiro Vitor Martins.

Stomata are tiny pores located in the leaf epidermis of almost all vascular land plants, responsible for the majority of gaseous diffusion between the bulk atmosphere and the leaf internal environment. The stomatal pore is surrounded by guard cells, which increase and decrease in volume in response to endogenous and external stimuli. In particular, fluctuations in leaf-to-air vapor pressure deficit (VPD) dictate daytime stomatal aperture and hence leaf gas exchange and hydration. Here we test whether abscisic acid (ABA) is primal in regulating stomatal response to VPD in osmotically adjusted herbs (Helianthus annuus and Glycine max); or whether the influence of the steady-state leaf water potential (Ψ_l) overcomes the hormonal control. We further examined the capacity of sunflower (H. annuus) leaves to acclimate to reduced water availability by modifying the sensitivity of xylem and stomata to soil water deficit. Stomatal aperture during VPD transitions was not associated with steady-state Ψ_l per se, rather stomatal closure under high VPD and stomatal hysteresis on returning to low VPD were closely linked with foliar ABA levels. We further indicate that ABA production under high VPD is triggered by changes in the leaf turgor pressure, and not by changes in Ψ_l per se. The osmotically adjusted sunflower plants also demonstrated a prolongation of stomatal opening as soil dried and a reduced sensitivity of photosynthesis to drought-induced damage. At the same time, the vulnerability of midrib xylem to cavitation was observed to be highly responsive to growth conditions, with water-limited plants producing conduits with thicker cell walls which were much more resistant to cavitation. Coordinated plasticity in osmotic potential and xylem vulnerability enabled water-limited sunflowers to safely extract water from the soil, while protecting leaf xylem against embolism. High plasticity in sunflower xylem vulnerability contrasts with data from woody plants, and may suggest an alternative strategy in herbs to cope with drought.

GENERAL INTRODUCTION

Plants frequently face challenging situations within their life span, particularly adverse water scarcity conditions that have been aggravated by the global climate changes (Sheffield et al., 2012). The hydraulic perturbation, driven by either soil water shortage or enhanced vapor pressure deficit between the leaf and the atmosphere (VPD), is a well-recognized factor that strongly negative impacts crop growth and production trough changing stomatal aperture, resulting in a major threat to food security (Foley et al., 2011). Stomata are tiny pores located in the leaf epidermis of almost all vascular land plants (Edwards and Axe, 1992), which present the conspicuous feature of opening and closing (Darwin, 1898) in response to a number of environmental stimuli. Light, which drives photosynthesis either in the mesophyll or in guard cell itself, is the strongest signal for stomatal opening (Brodribb and McAdam, 2017). In addition, reduced humidity conditions rapidly trigger stomatal closure yet in the presence of light. This leads to the reasonable conclusion that one of the primary stomatal functions is actively close the pore during water deficit as a means of protecting tissues from desiccation (Brodribb and McAdam, 2017).

Two main mechanisms are responsible for stomatal closure under high VPD; the passive hydraulic in ferns, lycophytes and conifers (Brodribb and McAdam, 2011), and the abscisic acid (ABA)-mediated closure in angiosperms (McAdam and Brodribb, 2015). Regarding the first mechanism, declining leaf water content under drought has a direct effect on guard cell turgor, which in turn reduces stomatal aperture (Brodribb and McAdam, 2011). Such passive mechanism is feasible in the above-cited basal groups since they lack subsidiary cells. The mechanical advantage of epidermal cells over guard cells in angiosperms, however, renders stomata to open transiently, instead of closing, in response to declining leaf water content, namely ‘wrong way’ response (Buckley, 2005). With regard to the ABA-mediated mechanism in angiosperms, it has been recently reported that foliar ABA levels considerably increase in angiosperms under high VPD conditions (McAdam and Brodribb, 2015), resulting in fast stomatal closure and protecting plants from desiccation. Nonetheless, this mechanism has been challenged by observations of functional VPD responses in mutants with impaired ABA synthesis or signaling (Merilo et al., 2017). Whichever the mechanism,

stomatal closure under high VPD is likely to protect important hydraulic anatomical elements (i.e. xylem conduits) from cavitation and consequent embolism.

Plant water transport through xylem cells is free of metabolic costs, however, the instability of water at high tensions results in an inevitable consequence: a vulnerability of the xylem to cavitation (Sperry & Tyree 1988). Cavitation occurs when tensions generated in the xylem vasculature can exceed a limit (i.e. 'air-seeding' threshold) where an air bubble is pulled into the conduit lumen. Such tiny bubbles, when inside the xylem conduits, rapidly expand to block the conduit to water flow (i.e. embolism; Tyree & Sperry 1989). Drought-induced embolism reduces the plant hydraulic conductances, negatively affecting important physiological process, such as photosynthetic gas exchanges (Sack & Holbrook 2006; Brodribb et al. 2007). The xylem vulnerability to cavitation emerges therefore as a primary constraint on vascular plant-function (Tyree & Sperry 1989); however, the plasticity of xylem vulnerability in herbaceous species remains unclear. It is also yet to be tested whether major changes in VPD are indeed sufficient to induce xylem embolism in angiosperm species.

Given the facts described above, we propose to examine (i) whether passive hydraulic or ABA-mediated mechanism control stomatal aperture under high VPD in two herbaceous species; (ii) the signal for triggering foliar ABA production during VPD transitions in angiosperms; and (iii) the effect of pronounced VPD transitions on xylem embolism and coordinated acclimation of xylem and stomatal sensitivity to dehydration in soft herbs. The study was planned to be carried out in two independent experiments, which comprises the two chapters presented here. In the first chapter, we find support for the proposed role of foliar ABA in rapid stomatal aperture regulation when hydrated plants experience an increase in VPD. Importantly, we demonstrate that although osmotic adjustment completely breaks the association between steady-state leaf water potential and stomatal conductance, a strong association between foliar ABA with stomatal conductance remains during VPD transitions. In the second chapter, we support fast stomatal closure under high VPD as an important mechanism for preventing xylem embolism and consequent loss of hydraulic conductance in angiosperms in a similar way to what occurs in basal land plants (Martins et al., 2016). We further demonstrate a clear coordinated acclimation of xylem and stomatal sensitivity to dehydration in osmotically adjusted sunflowers.

REFERENCES

Buckley, TN (2005) The control of stomata by water balance. New Phytologist 168: 275–292.

Brodribb TJ, Feild TS, Jordan GJ (2007) Leaf maximum photosynthetic rate and venation are linked by hydraulics. Plant Physiology 144: 1890–1898.

Brodribb TJ, McAdam SAM (2011) Passive origins of stomatal control in vascular plants. Science 331: 582–585.

Brodribb TJ, McAdam SAM (2017) Evolution of the stomatal regulation of plant water content. Plant Physiology 174: 639–649.

Darwin F (1898) Observations on stomata. Proceedings of the Royal Society 63: 413–417.

Edwards D, Axe L (1992) Stomata and mechanics of stomatal functioning in some early land plants. Cour. Forschungsinst. Senckenberg 147: 59–73.

Foley JA, Ramankutty N, Brauman KA, Cassidy ES, Gerber JS, Johnston M, Mueller ND, O'Connell C, Ray DK, West PC, Balzer C, Bennett EM, Carpenter SR, Hill J, Monfreda C,

Martins SCV, McAdam SAM, Deans RM, DaMatta FM, Brodribb TJ (2016) Stomatal dynamics are limited by leaf hydraulics in ferns and conifers: results from simultaneous measurements of liquid and vapour fluxes in leaves. Plant Cell & Environment 39: 694–705.

McAdam SA, Brodribb TJ (2015) The evolution of mechanisms driving the stomatal response to vapour pressure deficit. Plant Physiology 167: 833–43.

Merilo E, Yarmolinsky D, Jalakas P, Parik H, Tulva I, Rasulov B, Kilk K, Kollist H (2017) Stomatal VPD response: there is more to the story than ABA. Plant Physiology, pp-00912.

Sack L, Holbrook NM (2006) Leaf hydraulics. Annual Review of Plant Biology 57: 361–381.

Sheffield J, Wood EF, Roderick ML (2012) Little change in global drought over the past 60 years. Nature 491: 435–438.

Sperry JS, Tyree MT (1988) Mechanism of water stress induced xylem embolism. Plant Physiology 88: 581–587.

Tyree MT, Sperry JS (1989) Vulnerability of xylem to cavitation and embolism. Annual Review of Plant Physiology and Plant Molecular Biology 40: 19–38.

CHAPTER 1

Osmotic adjustment reinforces the key role played by ABA in stomatal responses to vapor pressure deficit in two herbs

Short Title: ABA in stomatal closure under high VPD

Corresponding author:

Timothy J. Brodribb

University of Tasmania

Phone: +61 362261707

E-mail: timothyb@utas.edu.au

Osmotic adjustment reinforces the role played by ABA in stomatal responses to vapor pressure deficit

Amanda A. Cardoso[1,2], Timothy J. Brodribb[1,*], Fábio M. DaMatta[2], Scott A. M. McAdam[3]

[1]School of Biological Sciences, University of Tasmania, Hobart, Tasmania 7001, Australia

[2]Departamento de Biologia Vegetal, Universidade Federal de Viçosa, 36570-900 Viçosa, MG, Brazil

[3]Botany and Plant Pathology, Purdue University, West Lafayette, Indiana 47906, USA

Author contributions: T.J.B. designed the research; A.A.C., T.J.B. and S.A.M.M. designed the methods; A.A.C. performed experiments; A.A.C., T.J.B. and S.A.M.M. analysed data; A.A.C., T.J.B. and S.A.M.M. wrote the manuscript with contributions from F.M.D.

One-sentence summary: ABA mediates stomatal responses to VPD rather than a passive response of stomata to changes in leaf water potential during a shift in transpiration in osmotically adjusted herbs.

Funding information: This work was supported by the Australian Research Council [grants nos. DE140100946 (S.A.M.M.) and DP140100666 (T.J.B.)] and the Brazilian agency FAPEMIG [grant no. BDS-00404-15 (A.A.C.)].

Abstract

Dynamic variation of the stomatal pore in response to leaf-air vapor pressure deficit (VPD) constitutes a critical regulation of daytime gas exchange. Such stomatal responses to VPD have been associated with both foliar abscisic acid (ABA) and leaf water potential (Ψ_l), however causation remains a matter of debate. Here we test whether ABA is similarly primal in regulating stomatal response to VPD by inducing osmotic adjustment of leaves in two herbaceous species as a means of modifying the relationship between ABA production and Ψ_l. Stomatal aperture during VPD transitions was not associated with steady-state Ψ_l per se, rather stomatal closure under high VPD and stomatal hysteresis on returning to low VPD were closely linked with foliar ABA levels. We further provide evidence for similar stomatal sensitivity to ABA, and hence to VPD, between osmotically adjusted and well-watered herbs, despite differences in steady-state Ψ_l under high VPD. Our results are consistent with ABA-mediated stomatal responses to VPD rather than a passive response of stomata to changes in Ψ_l during a shift in transpiration.

Introduction

Stomata on the leaves of terrestrial plants regulate the flow of CO_2 and water between the leaf and the atmosphere, thereby controlling plant hydration and photosynthetic rate (Farquhar & Sharkey, 1982). Dynamic regulation of the stomatal pore therefore forms one of the primary controllers of atmospheric water and CO_2 fluxes, as well as dictating the efficiency with which plants use water (Lawson & Blatt, 2014), and the operational safety of plants with regard to avoiding damaging desiccation (Brodribb & McAdam, 2017). The most pervasive stomatal dynamics are responses to light and leaf-air vapor pressure deficit (VPD). Light responses are tied to the direct action of membrane-bound phototropins in guard cells and an integrated photosynthetic signal (Shimazaki et al., 2007), while responses to air humidity appear to be produced by changes in leaf hydration caused by changes in VPD (Mott & Parkhurst, 1991). Stomatal response to VPD is a critical determinant of the efficiency of water use by leaves and is the focus of this study.

Stomata close as VPD increases, thereby substantially moderating the impact of increased evaporative demand. The mechanism responsible for this response remains under debate, with a diversity of research supporting the involvement of passive (Mott et al., 1997; Brodribb & McAdam, 2011) and active processes (Bunce, 1996; Bauerle et al., 2004; Bauer et al., 2013; McAdam & Brodribb, 2015; Merilo et al., 2017). Understanding the mechanism regulating stomatal closure in response to increasing VPD is of considerable importance because attempts to increase the productivity of irrigated crops have identified VPD responses as a primary target for improvement (Sinclair et al., 2016).

Probably the best-supported mechanism proposed for stomatal response to VPD in angiosperms is via the action of the phytohormone abscisic acid (ABA) (McAdam & Brodribb, 2015). Following early work showing large increases in foliar ABA as leaf turgor in desiccating leaves fell close to zero (Pierce & Raschke, 1980), suggestions of ABA as the driver of stomatal responses to VPD (Bunce, 1996) have received support from studies quantifying hormone levels in leaves (Bauerle et al., 2004; Giday et al., 2013; McAdam & Brodribb, 2015). More recent work shows that the upregulation of ABA biosynthetic genes driven by changes in leaf turgor occurs in a timeframe of minutes, providing sufficiently fast

activity to explain the relatively rapid closing responses of stomata to step changes in VPD (McAdam et al., 2016; Sussmilch et al., 2017). However, a recent report monitoring gas exchange in ABA biosynthetic and signaling mutants suggests that passive processes dominate stomatal responses to VPD in angiosperms (Merilo et al., 2017).

If the suggestion that foliar ABA synthesis is critical for controlling the angiosperm stomatal response to VPD is correct, a sequence of causation should be demonstrable from (i) transpiration rate (E) leading to transient changes in leaf water potential (Ψ_l) and hence in cell volume, and (ii) leaf water potential close to the turgor loss point (Ψ_{tlp}) triggering ABA production and stomatal response. Assuming stomatal responses to VPD was ABA-mediated rather than being passively related to Ψ_l (Merilo et al., 2017), one would expect stomatal responses to VPD in osmotically adjusted plants should reflect changes in turgor (and ABA levels) rather than Ψ_l. Thus we could expect a conserved relationship between foliar ABA and stomatal conductance (g_s) during dynamic responses to VPD, rather than a conserved relationship between Ψ_l and g_s per se (Buckley et al., 2003). Support for the concept of ABA-mediated stomatal VPD response is evident in data from several species, demonstrating that stomata remain similarly sensitive to variations in VPD under drought (Pou et al., 2008; Rodriguez-Dominguez et al., 2016). However, an interaction between the stomatal sensitivity to ABA and Ψ_l has been speculated, and according to such assumptions the stomatal sensitivity to VPD should be more pronounced under drought due to lower Ψ_l (Tardieu & Davies, 1992). Here, we examine the pathway from increasing in E to the production of ABA during VPD transitions in leaves of two herbaceous species, manipulating Ψ_{tlp} to test the robustness of the theory that foliar ABA, rather than Ψ_l per se, close stomata under high VPD, and to test whether stomatal sensitivity to ABA relies on the leaf water status.

Individuals of the two common herbs Helianthus annuus and Glycine max were grown under either well-watered or water-limited conditions as a means of modifying the leaf osmotic potential at full turgor (Ψ_s) and, hence, the Ψ_{tlp} of leaves. Stomatal responses to VPD transitions in whole plants were recorded to determine how adaptation to a drier growth environment affected associations between leaf gas exchange, water potential, and foliar ABA levels. Three main questions were targeted in this study: (i) does steady-state Ψ_l or foliar ABA levels regulate the stomatal response to VPD?; (ii) does steady-state Ψ_l modulate

stomatal sensitivity to ABA, and hence to VPD?; and (iii) what is the possible physiological mechanism responsible for triggering foliar ABA production under high VPD?

Results

Growing H. annuus and G. max plants under water-limited conditions induced osmotic adjustment (lower Ψ_s; Table 1) in both species, and the magnitude of the adjustment was dependent on the water availability during growth. As plants of H. annuus experienced a more severe stress when water-limited [minimum soil water potential (Ψ_{soil}) c. -1.3 ± 0.1 MPa] compared with G. max (minimum Ψ_{soil} c. -0.4 ± 0.05 MPa), they displayed a greater osmotic adjustment (0.45 MPa in H. annuus against 0.13 MPa in G. max; Table 1). Ψ_{tlp} was also lower in H. annuus grown under water-limited conditions compared with plants grown under well-watered conditions (a difference of 0.33 MPa), but not statistically significant lower in G. max (yet a shift of 0.1 MPa; Table 1).

VPD transition in whole plants

The response of both well-watered and water-limited plants from both species to VPD was the same (Fig. 1, 2). Initially rapid increases in E due to the higher evaporative demand occurred, followed by a rapid decline due to pronounced stomatal closure. Transient declines in Ψ_l were observed 5 min after plants were exposed to high VPD; and foliar ABA levels increased. Despite osmotic adjustment, stomatal sensitivity to VPD for both species remained similar (Table 2).

Measured Ψ_l 5 min after the transitions at high VPD exceeded the threshold for ABA production in both well-watered and water-limited plants of H. annuus, but not in G. max (Fig. 1, 2). Through modelling the instantaneous decline in Ψ_l over the first few minutes following the VPD transition (Supplemental Fig. S1), we found that the threshold Ψ_l to trigger ABA synthesis would have been reached before the fourth minute in G. max. This modelling approach demonstrated that in both species Ψ_l dropped below the trigger for ABA synthesis, and such transient Ψ_l is consistent with the measured accumulation of foliar ABA level under high VPD, yet by 5 min after the VPD transition the Ψ_l in G. max had already recovered above the ABA synthesis trigger threshold due to stomatal closure.

On returning to low VPD, a relatively fast, yet hysteretic, recovery in g_s was observed for both well-watered and water-limited plants of H. annuus, following rapid declines in foliar ABA levels to the original contents (no significant differences at 20 min after returning to low VPD) (Fig. 1, 2). On the other hand, incomplete reductions in foliar ABA levels were observed following a return to low VPD in both well-watered and water-limited plants of G. max, stabilizing c., three times higher than the original levels. The high foliar ABA levels after returning to low VPD resulted in a strongly hysteretic stomatal response in this species, which scarcely recovered over the time of measurement (Fig. 1, 2).

Regulating stomata during VPD transitions

No significant relationship between steady-state Ψ_l and g_s was observed during the VPD transitions for any tested species (Fig. 3A). By contrast, g_s during the VPD transitions was clearly regulated by changes in foliar ABA levels for both species. This includes stomatal closure under high VPD, and the reopening of stomata on returning to low VPD (Fig. 3B). Furthermore, the stomatal sensitivity to foliar ABA, during the VPD transitions, was similar between well-watered and water-limited plants for both species, despite considerable differences in the steady-state Ψ_l under high VPD (Table 2).

No consistent variation in plant hydraulic conductance (K_{plant}) was observed during or after VPD transitions in H. annuus plants (Supplemental Fig. S2). In G. max, however, there was a consistent decline in K_{plant} both during the increase and subsequent decrease in VPD, despite the full recovery of Ψ_l after returning to low VPD (Supplemental Fig. S2). This steady reduction in K_{plant} in G. max was found in both well-watered and water-limited plants.

VPD transition in single leaves

When single leaves from plants grown under well-watered conditions were exposed to a step increase in VPD, the stomata rapidly opened (by between 50% and 100%), due to a pronounced hydropassive, wrong-way response in both H. annuus and G. max (Fig. 4). As soon as 5 min after the VPD transition, a relatively slow stomatal closure took place, until g_s had either returned to very close to the initial values in a mild VPD transition from 1.0 to 2.0 kPa, or dropped to values c. 25% lower than the original ones in a severe VPD transition from 1.0 to 3.5 kPa (Fig. 4). When single leaves of each species were exposed to a mild step

increase in VPD, the maximum E were c. two times higher than the initial values, and when leaves were exposed to a severe step increase in VPD, the maximum E was c. five or four times higher than the initial steady-state in H. annuus and G. max, respectively. As soon as stomata started to close, E declined, and in all cases, stabilized at a higher level than initial (Fig. 4). Under a VPD of 2.0 kPa, foliar ABA levels in both species were similar to that measured under a VPD of 1.0 kPa. On the other hand, under a VPD of 3.5 kPa, foliar ABA levels were c. two times higher than at 1.0 kPa in both species (Fig. 4). Increases in ABA levels were only observed in leaves exposed to a VPD of 3.5 kPa, in which E transiently breached the threshold E (as calculated from the relationship between foliar ABA levels vs. Ψ_l in Fig. 5 and Equation 1, where F was considered equal to E), yet stomatal closure resulted in a steady-state E below this threshold line (Fig. 4). The increase in foliar ABA level in both species was consistent with the observed stomatal closure under high VPD (Fig. 4).

The relationship between Ψ_{tlp} and foliar ABA level

In well-watered plants, lowering the Ψ_l of excised leaves close to Ψ_{tlp} by bench dehydration was found to stimulate major foliar ABA production in both H. annuus and G. max (Fig. 5). Likewise, the threshold Ψ_l for major foliar ABA biosynthesis in osmotically adjusted plants for both species was observed to shift close to the new Ψ_{tlp} (Fig. 5).

Discussion

The mechanism driving stomatal closure in response to elevated VPD remains controversial (McAdam & Brodribb 2016; Merilo et al., 2017). Here we find support for the proposed role of foliar ABA in rapid stomatal aperture regulation when hydrated plants experience an increase in VPD. Importantly, we demonstrate that although osmotic adjustment completely breaks the association between steady-state Ψ_l and g_s (Fig. 5A), a strong association between foliar ABA and g_s remains during VPD transitions (Fig. 5B).

Foliar ABA levels define stomatal movement in response to VPD regardless of leaf water status

Our investigations present increases in foliar ABA levels as a functional short-term response, which play a crucial role in stomatal closure when both leaves (Fig. 4) and whole plants (Fig. 1, 2) are exposed to high VPD. Most importantly, we identified subtle augmented

levels of ABA as functionally relevant to induce stomatal closure in response to reduced air humidity (Fig. 4). This observation is consistent with recent quantitative assessments of increased foliar ABA levels across a diversity of angiosperms exposed to high VPD (McAdam & Brodribb, 2015; McAdam et al., 2015; McAdam & Brodribb, 2016) as well as the sensitivity of stomata from isolated epidermis to exogenous ABA (Raschke, 1987). Such low levels of ABA only require a short time frame to be synthesized in leaves, leading to a fast and efficient response mechanism, which restricts water loss and prevents pronounced declines in water status under reduced air humidity. Furthermore, by inducing osmotic adjustment and thus differences in the leaf water potential, we demonstrate that the stomatal sensitivity to ABA, and hence VPD, was not affected by the leaf water status. Instead, ABA appeared to be similarly primal regulating stomatal response to VPD in well-watered and osmotically adjusted herbs, despite considerable differences in steady-state Ψ_l (Table 2; Fig. 3B). This result challenges the view that epidermal water relations act as a modulator of the stomatal responses to ABA in vivo (Tardieu & Davies, 1992), and is difficult to explain by a purely passive regulation of stomata in response to VPD as observed in basal land plant lineages as hypothesised to regulate stomatal responses in angiosperms (Merilo et al., 2017).

Unlike other vascular land plants, angiosperm responses to VPD are typically hysteretic in terms of a relatively slow dynamic recovery of g_s when moving from high to low VPD (O'Grady et al., 1999; McAdam & Brodribb, 2015). Within this group of land plants, dynamic hysteresis is thought to result from slow catabolism of ABA accumulated under low humidity (McAdam & Brodribb, 2015), and our ABA recovery data support the idea that g_s recovery after returning to low VPD is strongly influenced by the levels of ABA (Fig. 1, 2, 3B). Regarding why foliar ABA levels remain high after returning to low VPD, previous studies suggest that the slow reduction in ABA levels is likely to be due to remaining high levels of transcript levels of NCED genes, as well as slow ABA catabolism (McAdam & Brodribb, 2015). However, we show that despite similar rates of ABA degradation (calculated during 60 min after returning to high humidity; Fig. 1, 2), the magnitude of hysteresis between H. annuus and G. max are remarkably different. The main difference between both species remains in the levels of ABA accumulated under high VPD. These results suggest that not only the rates of ABA catabolism influence the hysteretic recovery

of g_s of angiosperms after returning to low VPD as previously thought (McAdam & Brodribb, 2015; McAdam et al., 2016), but also the level of ABA accumulated under high VPD influences hysteresis within this group. In this respect we also suggest that the slightly increased level of ABA sufficient to induce stomatal closure provides an additional benefit in terms of requiring a shorter time frame to complete ABA catabolism, leading to a more rapid recovery of stomata aperture after returning to optimal humidity conditions.

Interestingly, hysteresis in G. max plants may also be associated with a systematic decline in K_{plant} after VPD was increased, which continued to decline following return to low VPD (Supplemental Fig. S2). This behavior contrasts with previous data suggesting stasis in hydraulic conductance when G. max was exposed to a step rise in VPD (Bunce, 2006), and is also at odds with the variable response of K_{plant} found here in H. annuus. However, an association between high ABA levels and depressed hydraulic conductance has been suggested (Pantin et al., 2013), and this cannot be ruled out as contributing to the sustained depression of g_s following a return to low VPD in G. max.

Cell volume as a trigger for foliar ABA production during VPD transitions

By bench-drying single leaves and using a high-precision method for ABA quantification, we indicate a distinct Ψ_l at or near Ψ_{tlp} that strongly induces foliar ABA biosynthesis in both herbaceous species (Fig. 5) in good agreement with prevailing literature (Zabadal, 1974; Beardsell & Cohen, 1975; Pierce & Raschke, 1980; Davies et al., 1981; Creelman & Zeevaart, 1985). Recent work has shown that changes in cell volume, most pronounced as the leaf nears Ψ_{tlp}, triggers foliar ABA biosynthesis (McAdam & Brodribb, 2016; Sussmilch et al., 2017; Sack et al., 2017). This seems a likely pathway connecting changes in transpiration, caused by VPD, with ABA production. Although, we clearly indicate that the steady-state Ψ_l per se is not primarily associated with stomatal aperture during the VPD transitions (Fig. 3A), we strongly suggest that the transient declines in Ψ_l within the first minutes of the step increase in VPD play an important role in mediating ABA production. Indeed cell volume does seem to be the main trigger for ABA biosynthesis as we observed a subtle increase in the levels of foliar ABA under high VPD when leaves experienced Ψ_l above a complete loss of leaf turgor (compare threshold Ψ_l in Fig. 1, 2 with Ψ_{tlp} in Table 1).

Materials and Methods

Plant material and growth conditions

Individuals of H. annuus cv. Yellow Empress (Asteraceae) and G. max cv. Bunya (Fabaceae), were grown for c. 60 days under two contrasting conditions, i.e. well-watered or water-limited conditions. Well-watered plants were grown inside a controlled glasshouse regulated at 16-h day at 25°C/15°C day/night temperatures, VPD at c. 1.0 kPa during the day and natural light [maximum photosynthetic photon flux density (PPFD) of 1500 µmol m^{-2} s^{-1} at the pot surface]. Plants were grown in c. 3 L plastic pots filled with potting mix and watered daily to full capacity (Ψ_{soil} > –0.3 MPa). Water-limited plants were grown outside the glasshouse during summer (from December 2016 to January 2017) under a natural c. 16-h day at c. 23°C/13°C day/night temperatures, VPD at 1.45 ± 0.7 kPa during the day, and natural light (maximum PPFD of 1800 µmol m^{-2} s^{-1} at the pot surface). Plants were grown in c. 3 L plastic pots filled with potting mix and watered three times per week to full capacity leading to oscillations in Ψ_{soil} ranging from –0.5 ± 0.1 MPa to –1.3 ± 0.1 MPa for plants of H. annuus, and from –0.3 ± 0.01 MPa to –0.4 ± 0.05 MPa for G. max (Table 1). The Ψ_{soil} was assessed measuring the Ψ_l of plants before sunrise (0600 h) using a Scholander pressure chamber (615D, PMS Instrument Company, Albany, USA).

Physiological traits responses to growth conditions

Three c. 60-day-old individuals for each species grown under either glasshouse or field conditions were used to assess Ψ_{tlp}, Ψ_s, leaf hydraulic conductance (K_{leaf}) and leaf capacitance (C_{leaf}). At the end of the 60 days, both well-watered and watered-limited plants of H. annuus were c. 100–120 cm tall, and of G. max were c. 60-80 cm tall; and each plant had c. 20 leaves. All measurements were carried out using fully expanded leaves developed entirely during the treatment period.

Ψ_{tlp} and C_{leaf} were determined by the relationship between Ψ_l and water volume in the leaf (pressure-volume analysis; Tyree & Hammel, 1972). Leaves were cut under water and rehydrated overnight until Ψ_l was > –0.1 MPa. Leaf weight and Ψ_l were measured over time during slow desiccation on the laboratory bench until Ψ_l began to rise due to cell damage. Ψ_{tlp} was determined as the point of inflection between the linear (pre-turgor loss)

and nonlinear (post-turgor loss) portions of the relative water content and Ψ_l relationship, and the C_{leaf} was calculated in terms of relative water content from the linear slope of the plot and normalized by leaf area according to Blackman & Brodribb (2011).

Measurements of Ψ_s were carried out using a stem psychrometer (PSY1, ICT International, Armidale, Australia) in a similar way to Bartlett et al. (2012). Leaf discs of c. 5 mm diameter were sampled from hydrated leaves, wrapped in tin-foil, and immediately frozen in liquid nitrogen to disrupt cell walls and eliminate turgor pressure. Midribs and large veins were avoided in selecting the leaf discs. The tissues were then sealed in a stem psychrometer, and the Ψ_s (Ψ_l is here considered Ψ_s due to absence of turgor pressure) logged every 10 min until stable (c. 30 min).

The K_{leaf} was assessed by the evaporative flux method (Sack et al., 2002; Brodribb & Holbrook, 2006) using a custom-built flowmeter. Well-watered individuals were transferred to the laboratory and bagged overnight (initial Ψ_l c. –0.3 MPa). During the morning, three leaves were acclimated to high humidity and light and low CO_2 (bagged with nitrogen and wet paper) for at least 30 min to ensure high g_s. They were then cut under water, and immediately connected to the flowmeter. A light source (providing PPFD of c. 600 μmol m^{-2} s^{-1}) and a constant stream of warm air were applied to the leaves producing rates of flow c. 5 mmol m^{-2} s^{-1}. After flow reached a steady-state, the Ψ_l was measured using a Scholander pressure chamber. Calculation of K_{leaf} was made using the equation:

$$K_{leaf} = F \times \Psi_l^{-1} \quad (1)$$

where F is the water flow into the leaf (normalized to leaf area, determined by a flatbed scanner), and Ψ_l was measured at steady-state. Values were normalized to the viscosity of water at 20°C (Korson et al., 1969).

VPD transitions in whole plants

Experiments were conducted by exposing whole individuals grown either under well-watered or water-limited conditions to rapid VPD transitions in growth cabinets. All plants were watered and acclimated overnight in a custom-built chamber under dark and low VPD conditions [0.5 ± 0.2 kPa (30°C and 88% relative humidity) for plants grown under well-watered conditions or 1.0 ± 0.1 kPa (30°C and 76% relative humidity) for plants grown under

water-limited conditions]. During the next morning the light was turned on at room ambient PPFD of c. 300 μmol m^{-2} s^{-1}, and after c. 90 min leaf gas exchange, Ψ_l and foliar ABA levels were measured. Next, plants were immediately transferred to a growth chamber under high VPD [3.0 ± 0.1 kPa (30°C and 29% relative humidity) for plants grown in the well-watered condition or 3.5 ± 0.1 kPa (30°C and 18% relative humidity) for plants grown in water-limited condition] with the low humidity sustained by a condensing dehumidifier (SeccoUltra 00563, Olimpia-Splendid, Gualtieri, Italy). The Ψ_l was assessed at 5 and 60 min after the increase in VPD; leaf gas exchange at 10, 20, 40 and 60 min after; and tissue was harvested for foliar ABA analysis 60 min after. The plants then returned to the low VPD condition, and Ψ_l was assessed at 60 min after the decrease in VPD; leaf gas exchanges and tissue for foliar ABA analysis was taken at 20, 40 and 60 min after this transition from high to low VPD. Air relative humidity were monitored every 30 s during the experimental period using a humidity probe (HMP45AC, Vaisala, Helsinki, Finland). Air and leaf temperature were measured using a thermocouple shielded from radiation and connected to a data logger (CR800, Campbell Scientific, Logan, USA).

For each species and growth condition, three individuals were used for each VPD transition. One fully expanded leaf per plant was selected for the gas exchange measurements which were performed using a portable photosynthesis equipment (GFS-3000, Heinz Walz, Effeltrich, Germany). Conditions in the cuvette were controlled at temperature of 30°C, 390 μmol CO_2 mol^{-1} air, PPFD of 1000 μmol m^{-2} s^{-1} at the leaf surface and the VPD was maintained as close as possible to the ambient VPD. Instantaneous E was calculated using g_s (obtained from the gas exchange measurements) and VPD (obtained from the relative humidity of the air chamber and leaf temperature measured with a thermocouple). One leaf per plant was randomly sampled for Ψ_l at each measurement time. After harvesting, leaves were wrapped in wet paper towel, bagged and placed in an ice box for Ψ_l assessment using a Scholander pressure chamber.

The adjacent leaf to the one used for gas exchange measurements was harvested for foliar ABA quantification. The same leaf was harvested (c. 5 cm^2) at different measurement times to avoid age differences in ABA levels. For the initial foliar ABA levels, three other random leaves were sampled to determine variation in the ABA levels in the plant (i.e. n = 6

leaves). For foliar ABA assessment, leaf samples were weighted (± 0.0001 g; MS204S, Mettler-Toledo, Greifensee, Switzerland), immediately covered with cold (–20°C) 80% (v/v) methanol in water with 250 g L^{-1} (m/v) of added butylated hydroxytoluene, and stored at –20°C. Samples were purified and foliar ABA levels were then quantified by physicochemical methods with an added internal standard by ultra-performance liquid chromatography tandem mass spectrometry (UPLC-MS) according to McAdam (2015). Reference lines regarding the minimum Ψ_l to trigger foliar ABA production consistent with the level measured under high VPD were determined using the relationship between ABA level and Ψ_l (as described in the "Foliar ABA accumulation by bench dehydration" section).

Using g_s and ABA levels, and g_s and steady-state Ψ_l data from VPD transitions of whole plants from each species, we fitted a relationship between these parameters using the curve-fitting function of the Sigma Plot software.

Calculation of K_{plant} was made under steady-state VPDs using the equation:

$$K_{plant} = E \times \Psi_l^{-1} \quad (2)$$

To use this approach, the Ψ_{soil} was assumed to be close to zero, since all plants, including the water-limited ones, were watered in the night before the experiment.

Modelling Ψ_l of whole plants exposed to VPD transitions

The dynamic drop in Ψ_l in the first 240 s after the whole plant transition from low to high VPD was modelled assuming that leaf dehydration is equivalent to the discharging of a capacitor through a resistor (Brodribb & Holbrook, 2003) using the following equation:

$$\Psi_{l,\,i+1} = \Psi_{l,i} - [\Psi_{min} - (\Psi_{min} \times e^{\frac{-t \times K_{plant}}{C_{leaf}}})] \quad (3)$$

where $\Psi_{l,i}$ (MPa) is the steady-state Ψ_l under low VPD; Ψ_{min} (MPa) is the minimum Ψ_l that would be reached at steady-state conditions under high VPD, considering the maximum E (E_{max}; mmol m^{-2} s^{-1}; driven by the initial g_s and high VPD) and unit for K_{plant} is mmol m^{-2} s^{-1} MPa^{-1}, calculated as $\Psi_{min} = E_{max} \times K_{plant}^{-1}$; t is the time interval (s); and unit for C_{leaf} is mmol m^{-2} MPa^{-1}.

VPD transitions in single leaves

Experiments were conducted by exposing single leaves to two different rapid VPD transitions (a mild and a severe transition in VPD) in a cuvette. For each species and VPD transition, three leaves from three individuals were examined. Plants grown under well-watered condition were fully watered and bagged overnight to avoid ABA production before beginning experiments. During the next day, two fully expanded leaves for each individual (one for each VPD transition) were enclosed in an 8-cm^2 cuvette connected to the portable photosynthesis system GFS-3000 while the rest of the leaves were still covered with wet papers. The initial conditions in the leaf cuvette were regulated at constant 20°C (for the mild VPD transition) or 30°C (for the severe VPD transition), 390 μmol CO_2 mol^{-1} air, PPFD of 1000 μmol m^{-2} s^{-1} at the leaf surface and VPD of 1.0 ± 0.1 kPa. Leaves remained at the initial condition until leaf gas exchange had reached a maximum. The VPD was then rapidly increased (over c. 2 min) either to 2.0 ± 0.2 kPa or 3.5 ± 0.1 kPa and it was maintained until leaf gas exchange had stabilized under the high VPD condition. Leaf gas exchange was logged every 60 s to build the kinetics of the stomatal and transpiration response. Because of differences in equilibration time between the reference and sample infrared gas analysers, data from the first 3 min immediately after the VPD transition were discarded.

Harvesting of leaf tissue for ABA levels were undertaken just before the increase in VPD on the portion of the leaf covered with wet paper and maintained in dark outside the cuvette, and at the end of the VPD transition on the portion of leaf that was inside the cuvette. Foliar ABA was assessed as described above. The ABA levels measured under 3.5 kPa were used to calculate threshold Ψ_l for foliar ABA production (for further information, see "Foliar ABA Accumulation by Bench Dehydration" section), and dynamics in Ψ_l associated with changes in E were calculated based on measured K_{leaf} (Equation 1).

Foliar ABA accumulation by bench dehydration

In order to determine the relationship between Ψ_l and ABA levels we monitored foliar ABA in excised leaves during desiccation. For each species and growth condition, three plants were bagged with wet paper towels and put in the dark overnight. Early in the morning, one leaf from each individual was excised and left to dry slowly (initially under two sheets of wet paper towel to slow the dehydration, and after Ψ_{tlp} without wet paper) on a bench at

22°C and low light (PPFD of c. 30 μmol m^{-2} s^{-1}). During the course of the next 12 h, Ψ_l and ABA levels were assessed c. 15 times for the same leaf. Leaf discs of c. 5 mm diameter were sampled, enclosed in a stem psychrometer and the Ψ_l was logged every 10 min until stable (c. 90 min). Immediately after sampling the leaf for Ψ_l, harvesting of leaf tissue for ABA levels were undertaken as described above. Approximately 20% of the each leaf area was removed for this experiment. The relationship between foliar ABA level and Ψ_l for each species and growth conditions were fitted, and the equation obtained using the curve-fitting function of the Sigma Plot software. The threshold Ψ_l for foliar ABA production consistent with values measured under high VPD were calculated using these equation.

Statistical analysis

To test changes in foliar ABA level over the VPD transition, Student's t test were performed between each foliar ABA level (n = 3) and the initial value (n = 6), as well as to test whether the growth conditions affected the measured physiological parameters, Student's t test (n = 3) was performed within each species.

Acknowledgements

We gratefully acknowledge CSIRO Hobart for stem psychrometers used during the experiments.

Competing financial interests

The authors declare no competing financial interests.

Tables

Table 1. Range of soil water potential (Ψ_{soil}; –MPa) and mean values (n = 3, ± SE) for leaf water potential at turgor loss point (Ψ_{tlp}; –MPa), leaf osmotic potential at full turgor (Ψ_s; –MPa), leaf hydraulic conductance (K_{leaf}; mmol m^{-2} s^{-1} MPa^{-1}) and leaf capacitance (C_{leaf}; mmol m^{-2} MPa^{-1}) in Helianthus annuus and Glycine max plants grown under either well-watered or water-limited conditions.

Parameters	Helianthus annuus		Glycine max	
	Well-watered	Water-limited	Well-watered	Water-limited
Ψ_{soil}	0.0 – 0.3	0.5 – 1.3	0.0 – 0.3	0.3 – 0.4
Ψ_{tlp}	0.71 ± 0.03	1.04 ± 0.02**	0.99 ± 0.05	1.09 ± 0.01^{ns}
Ψ_s	0.50 ± 0.01	0.95 ± 0.05*	0.77 ± 0.03	0.90 ± 0.01*
K_{leaf}	11.88 ± 1.14	11.05 ± 0.16^{ns}	9.90 ± 0.31	8.72 ± 0.88^{ns}
C_{leaf}	3064 ± 102	3417 ± 211^{ns}	1444 ± 176	1849 ± 236^{ns}

Stars denote significant changes (Student's t test; ** $P < 0.01$, *$P < 0.05$, ns not significant) between growth conditions within species.

Table 2. Mean (n = 3, ± SE) sensitivity of stomatal conductance (g_s) to leaf-air vapor pressure deficit (VPD) and to foliar abscisic acid (ABA) levels [as represented by the difference in the percentage of g_s related to the difference in the VPD ($\Delta g_s/\Delta VPD$) or in the ABA levels ($\Delta g_s/\Delta ABA$)], and the mean (n = 3, ± SE) steady-state leaf water potential under high VPD ($\Psi_{l\_high\ VPD}$) in Helianthus annuus and Glycine max plants grown under either well-watered or water-limited conditions.

Parameters	Helianthus annuus		Glycine max	
	Well-watered	Water-limited	Well-watered	Water-limited
$\Delta g_s/\Delta VPD$	32.8 ± 0.8	33.6 ± 1.4^{ns}	32.0 ± 1.3	34.75± 1.7^{ns}
$\Delta g_s/\Delta ABA$	3.6 ± 1.0	3.5 ± 1.0 ^{ns}	1.3 ± 0.3	1.7 ± 0.2^{ns}
$\Psi_{l\_high\ VPD}$	–0.36 ± 0.05	–0.68 ± 0.04	–0.28 ± 0.02	–0.37 ± 0.01

^{ns} denotes not significant changes (Student's t test) between growth conditions within species.

Figure legends

Figure 1. Mean response of stomatal conductance, transpiration, leaf water potential and foliar ABA level in Helianthus annuus and Glycine max after whole plants (n = 3, ± SE, and n = 6, ± SE for initial ABA level) grown under well-watered condition were exposed to a step change in VPD from 0.5 kPa (white region) to 3.0 kPa (grey region) and then returning to 0.5 kPa (white region). Solid red lines indicate the minimum leaf water potential necessary to trigger the foliar ABA level accumulated under VPD of 3.0 kPa, calculated using the relationship between foliar ABA level and leaf water potential (see Fig. 5). Stars denote a significant change in foliar ABA level compared with the initial one (Student's t test; ** $P < 0.01$, * $P < 0.05$, ns not significant). ABA, abscisic acid; FW, fresh weight; VPD, leaf-air vapor pressure deficit.

Figure 2. Mean response of stomatal conductance, transpiration, leaf water potential and foliar ABA level in Helianthus annuus and Glycine max after whole plants (n = 3, ± SE, and n = 6, ± SE for initial ABA level) grown under water-limited condition were exposed to a step change in VPD from 1.0 kPa (white region) to 3.5 kPa (grey region) and then returning to 1.0 kPa (white region). Solid red lines indicate the minimum leaf water potential necessary to trigger the foliar ABA level accumulated under VPD of 3.5 kPa, calculated using the relationship between foliar ABA level and leaf water potential (see Fig. 5). Stars denote a significant change in foliar ABA level compared with the initial one (Student's t test; ** $P < 0.01$, * $P < 0.05$, ns not significant). ABA, abscisic acid; FW, fresh weight; VPD, leaf-air vapor pressure deficit.

Figure 3. The relationship between the mean (n = 3, ± SE) leaf water potential and stomatal conductance (A), and between foliar ABA level and stomatal conductance (B) in plants of Helianthus annuus (blue circles) and Glycine max (red circles) grown under either well-watered (filled circles) or water-limited (open circles) conditions during VPD transitions. The relationships in A are not significant. ABA, abscisic acid; FW, fresh weight; VPD, leaf-air vapor pressure deficit.

Figure 4. Mean response of stomatal conductance, transpiration rate and foliar ABA level in Helianthus annuus and Glycine max after single leaves (n = 3, ± SE) from plants grown under well-watered condition were exposed to a step change in VPD (grey region) from 1.0 kPa to

either 2.0 kPa (white symbols) or 3.5 kPa (black symbols). Solid red lines indicate the transpiration rate necessary to drop leaf water potential to a value consistent to the foliar ABA level found under VPD of 3.5 kPa, considering constant leaf hydraulic conductance (see Table 1) and the relationship between foliar ABA level and leaf water potential (see Fig. 5). ABA, abscisic acid; FW, fresh weight; VPD, leaf-air vapor pressure deficit.

Figure 5. Relationship between foliar ABA level and leaf water potential (black circles; n = 3) in plants of Helianthus annuus and Glycine max grown under either well-watered or water-limited conditions. Lowering the Ψ_l (-MPa) stimulates increase in foliar ABA level (ng g^{-1} FW) following the equations: ABA = exp ($7.2583 \times \Psi_l$) in H. annuus grown under well-watered condition, ABA = exp ($5.5523 \times \Psi_l$) in G. max grown under well-watered condition, ABA = exp ($5.0750 \times \Psi_l$) in H. annuus grown under water-limited condition and ABA = exp ($5.0218 \times \Psi_l$) in G. max grown under water-limited condition. Dashed grey lines indicate water potential at turgor loss point (mean; n = 3; see Table 1). ABA, abscisic acid; FW, fresh weight; Ψ_l, leaf water potential.

Supplemental Materials

Supplemental Figure S1. Modelled dynamic drop in leaf water potential during a step transition in leaf-air vapor pressure deficit.

Supplemental Figure S2. Plant hydraulic conductance during reversible sequence of leaf-air vapor pressure deficit transitions.

Literature Cited

Bartlett MK, Scoffoni C, Ardy R, Zhang Y, Sun S, Cao K, Sack L (2012) Rapid determination of comparative drought tolerance traits: using an osmometer to predict turgor loss point. Methods Ecol Evol 3: 880–888

Bauer H, et al. (2013) The stomatal response to reduced relative humidity requires guard cell-autonomous ABA synthesis. Curr Biol 23: 53–57

Bauerle WL, Whitlow TH, Setter TL, Vermeylen FM (2004) Abscisic acid synthesis in Acer rubrum L. leaves: a vapor-pressure-deficit-mediated response. J Am Soc Hortic Sci 129: 182–187

Beardsell MF, Cohen D (1975) Relationships between leaf water status, abscisic acid levels, and stomatal resistance in maize and sorghum. Plant Physiol 56: 207–212

Blackman CJ, Brodribb TJ (2011) Two measures of leaf capacitance: insights into the water transport pathway and hydraulic conductance in leaves. Funct Plant Biol 38: 118–126

Brodribb TJ, Holbrook NM (2003) Stomatal closure during leaf dehydration, correlation with other leaf physiological traits. Plant Physiol 132: 2166–2173

Brodribb TJ, Holbrook NM (2006) Declining hydraulic efficiency as transpiring leaves desiccate: two types of response. Plant Cell Environ 29: 2205–2215

Brodribb TJ, McAdam SAM (2011) Passive origins of stomatal control in vascular plants. Science 331: 582–585

Brodribb TJ, McAdam SAM (2017) Evolution of the stomatal regulation of plant water content. Plant Physiol 174: 639–649

Buckley TN, Mott KA, Farquhar GD (2003) A hydromechanical and biochemical model of stomatal conductance. Plant Cell Environ 26: 1767–1785

Bunce JA (1996) Does transpiration control stomatal responses to water vapour pressure deficit? Plant Cell Environ 20: 131–135

Bunce JA (2006) How do leaf hydraulics limit stomatal conductance at high water vapour pressure deficits? Plant Cell Environ 29: 1644–1650

Creelman RA, Zeevaart JAD (1985) Abscisic acid accumulation in spinach leaf slices in the presence of penetrating and nonpenetrating solutes. Plant Physiol 77: 25–28

Davies WJ, Wilson JA, Sharp RE, Osonubi O (1981) Control of stomatal behaviour in water-stressed plants. In PG Jarvis, TA Mansfield, eds, Stomatal Physiology. Cambridge University Press, Cambridge, pp 163–185

Farquhar GD, Sharkey TD (1982) Stomatal conductance and photosynthesis. Annu Rev Plant Biol 33: 17–45

Giday H, Fanourakis D, Kjaer KH, Fomsgaard IS, Ottosen CO (2013) Foliar abscisic acid content underlies genotypic variation in stomatal responsiveness after growth at high relative air humidity. Ann Bot 112: 1857–1867

Korson L, Drost-Hansen W, Millero FJ (1969) Viscosity of water at various temperatures. J Phys Chem 73: 34–39

Lawson T, Blatt MR (2014) Stomatal size, speed, and responsiveness impact on photosynthesis and water use efficiency. Plant Physiol 164: 1556–1570

McAdam SAM (2015) Physicochemical quantification of abscisic acid levels in plant tissues with an added internal standard by ultra-performance liquid chromatography. Bio Protoc 5: e1599.

McAdam SAM, Brodribb TJ (2015) The evolution of mechanisms driving the stomatal response to vapor pressure deficit. Plant Physiol 167: 833–843

McAdam SAM, Brodribb TJ (2016) Linking turgor with ABA biosynthesis: implications for stomatal responses to vapour pressure deficit across land plants. Plant Physiol 171: 2008–2016

McAdam SAM, Sussmilch FC, Brodribb TJ (2016) Stomatal responses to vapour pressure deficit are regulated by high speed gene expression in angiosperms. Plant Cell Environ 39: 485–491

McAdam SAM, Sussmilch FC, Brodribb TJ, Ross JJ (2015) Molecular characterization of a mutation affecting abscisic acid biosynthesis and consequently stomatal responses to humidity in an agriculturally important species. AoB Plants 7: plv091

Merilo E, Yarmolinsky D, Jalakas P, Parik H, Tulva I, Rasulov B, Kilk K, Kollist H (2017) Stomatal VPD response: there is more to the story than ABA. Plant Physiol, pp-00912

Mott KA, Denne F, Powell J (1997) Interactions among stomata in response to perturbations in humidity. Plant Cell Environ 20: 1098–1107

Mott KA, Parkhurst DF (1991) Stomatal responses to humidity in air and helox. Plant Cell Environ 14: 509–515

O'Grady AP, Eamus D, Hutley LB (1999) Transpiration increases during the dry season: patterns of tree water use in eucalypt open-forests of northern Australia. Tree Physiol 19: 591–597

Pantin F, Monnet F, Jannaud D, Costa JM, Renaud J, Muller B, Simonneau T, Genty B (2013) The dual effect of abscisic acid on stomata. New Phytol 197: 65–72

Pierce M, Raschke K (1980) Correlation between loss of turgor and accumulation of abscisic acid in detached leaves. Planta 148: 174–182

Pou A, et al. (2008) Adjustments of water use efficiency by stomatal regulation during drought and recovery in the drought-adapted Vitis hybrid Richter-110 (V. berlandieri × V. rupestris). Physiol Plant 134: 313–323

Raschke K (1987) Action of Abscisic acid on Guard cells. In E Zeiger, GD Farquhar, IR Cowan, eds, Stomatal Function. Stanford University Press, Stanford, pp 253–279

Rodriguez-Dominguez CM, Buckley TN, Egea G, de Cires A, Hernandez-Santana V, Martorell S, Diaz-Espejo A (2016) Most stomatal closure in woody species under moderate drought can be explained by stomatal responses to leaf turgor. Plant Cell Environ 39: 2014–2026

Sack L, John GP, Buckley TN (2017) ABA accumulation in dehydrating leaves is associated with decline in cell volume not turgor pressure. Plant Physiol, pp-01097

Sack L, Melcher PJ, Zwieniecki MA, Holbrook NM (2002) The hydraulic conductance of the angiosperm leaf lamina: a comparison of three measurement methods. J Exp Bot 53: 2177–2184

Shimazaki K, Doi M, Assmann SM, Kinoshita T (2007) Light regulation of stomatal movement. Annu Rev Plant Biol 58: 219–247

Sinclair TR, Devi JM, Carter TE (2016) Limited-transpiration trait for increased yield for water-limited soybean: from model to phenotype to genotype to cultivars. In Yin X, Struik, eds, PC Crop Systems Biology. Springer International Publishing, Switzerland, pp 129–146.

Sussmilch FC, Brodribb TJ, McAdam SAM (2017) Up-regulation of NCED3 and ABA biosynthesis occur within minutes of a decrease in leaf turgor but AHK1 is not required. J Exp Bot 68: 2913–2918

Tardieu F, Davies WJ (1992) Stomatal response to abscisic acid is a function of current plant water status. Plant Physiol 98: 540–545

Tyree MT, Hammel HT (1972) The measurement of the turgor pressure and the water relations of plants by the pressure-bomb technique. J Exp Bot 23: 267–282

Zabadal TJ (1974) A water potential threshold for the increase of abscisic acid in leaves. Plant Physiol 53: 125–127

Figure 1

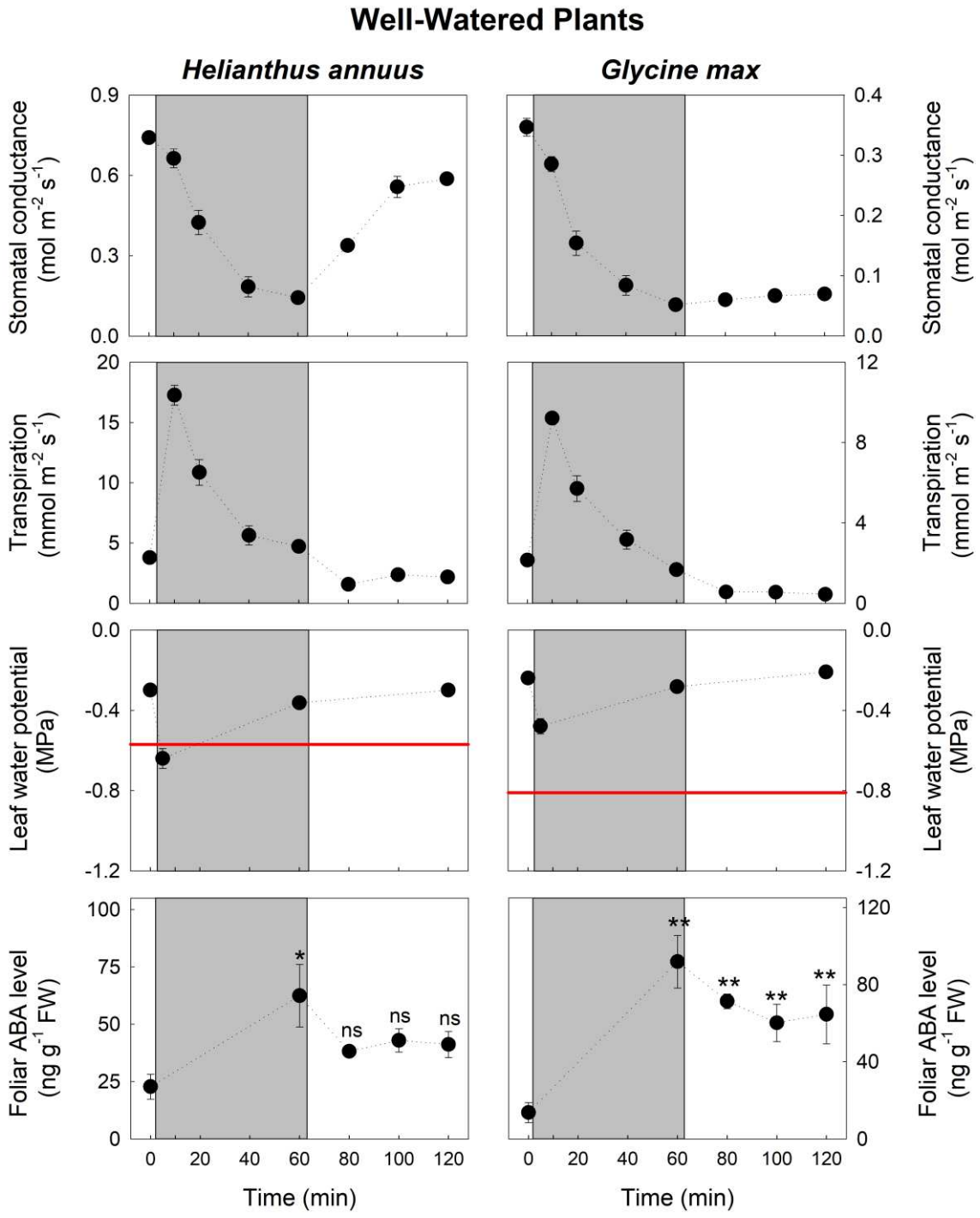
Well-Watered Plants
Helianthus annuus
Glycine max
Stomatal conductance (mol m-2 s-1)
Transpiration (mmol m-2 s-1)
Leaf water potential (MPa)
Foliar ABA level (ng g-1 FW)
Time (min)
ns
*
**

Figure 2

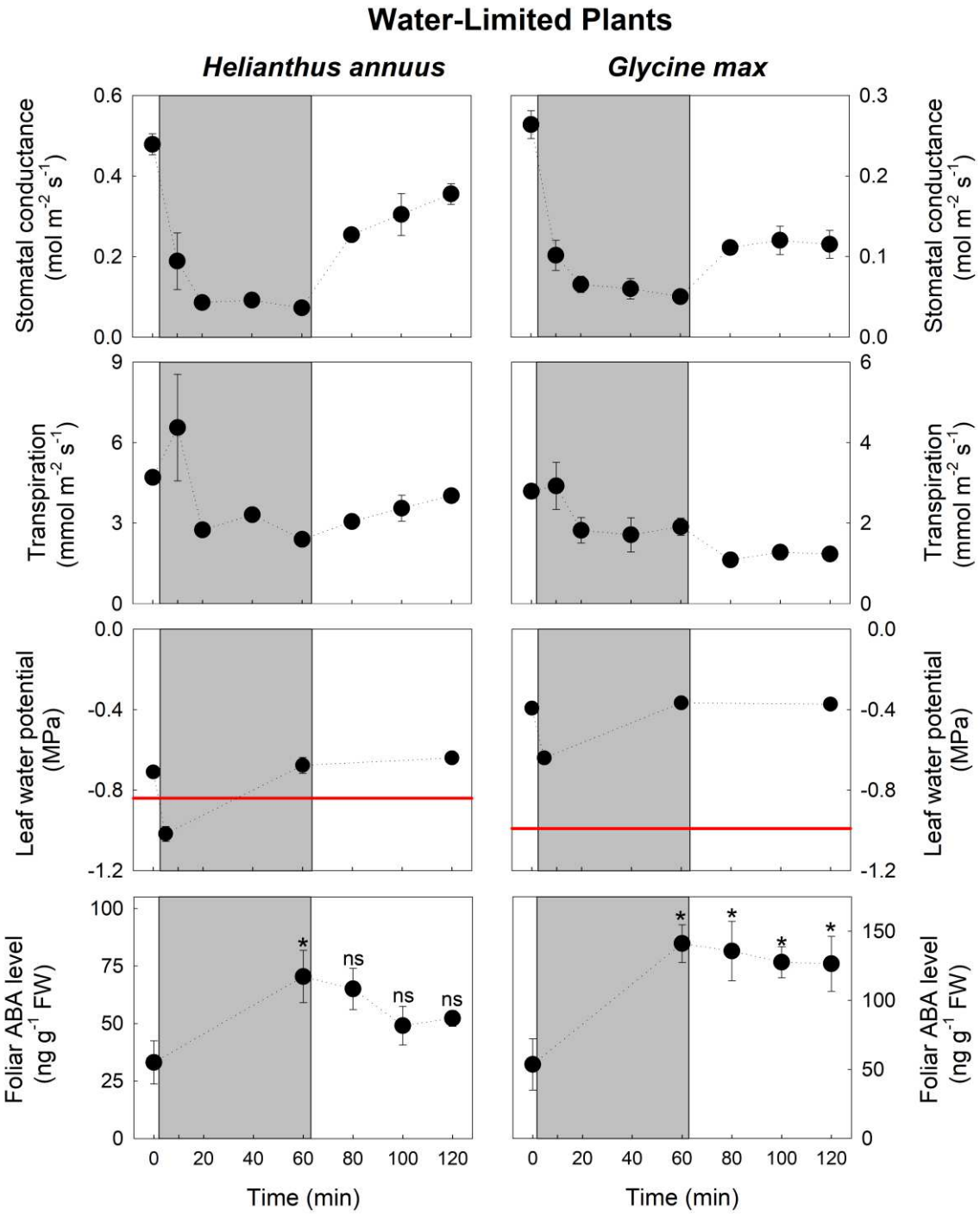
Water-Limited Plants
Helianthus annuus
Glycine max
Stomatal conductance (mol m-2 s-1)
Transpiration (mmol m-2 s-1)
Leaf water potential (MPa)
Foliar ABA level (ng g-1 FW)
Time (min)
ns
*

Figure 3

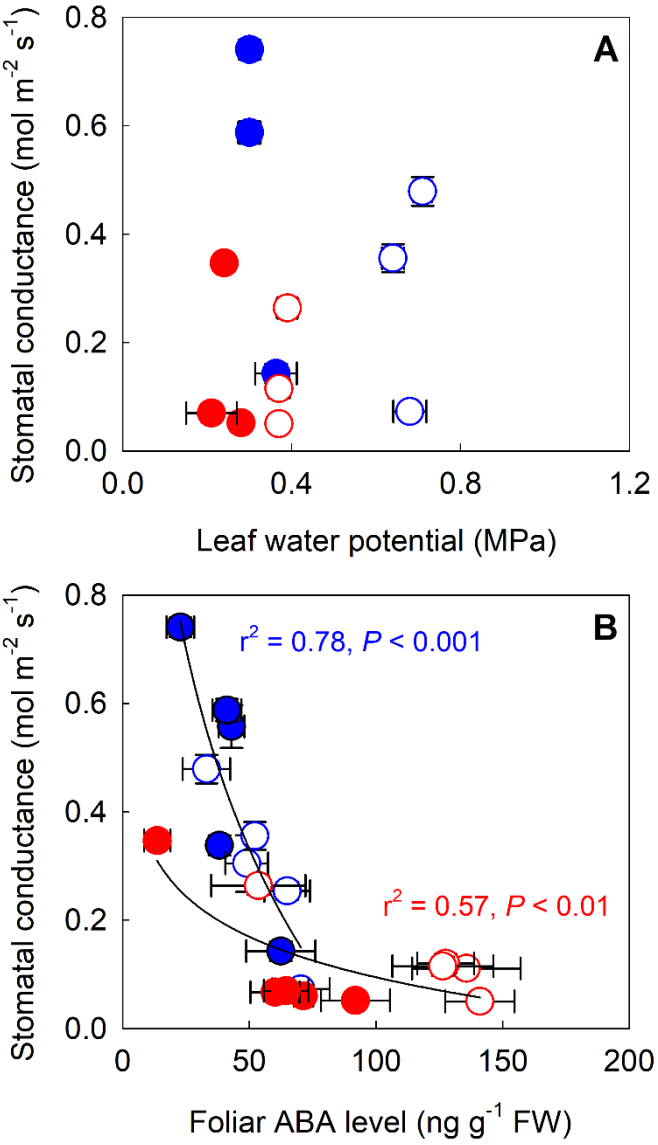
A
Stomatal conductance (mol m-2 s-1)
0.0
0.2
0.4
0.6
0.8
0.0
0.4
0.8
1.2
Leaf water potential (MPa)
B
r2 = 0.78, P < 0.001
r2 = 0.57, P < 0.01
Stomatal conductance (mol m-2 s-1)
0
50
100
150
200
Foliar ABA level (ng g-1 FW)

Figure 4

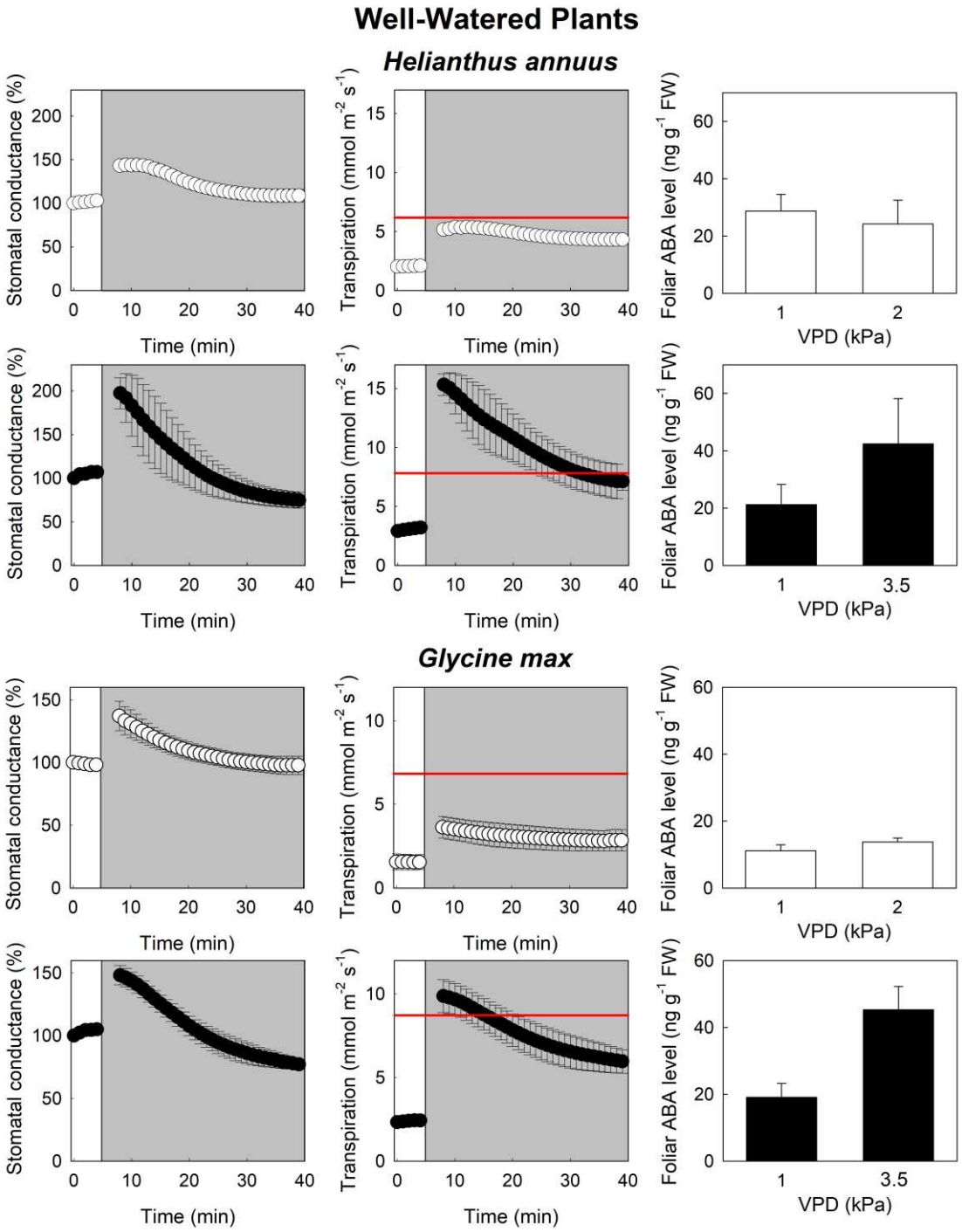
Well-Watered Plants
Helianthus annuus
Glycine max
Stomatal conductance (%)
Transpiration (mmol m-2 s-1)
Foliar ABA level (ng g-1 FW)
Time (min)
VPD (kPa)
1
2
3.5

Figure 5

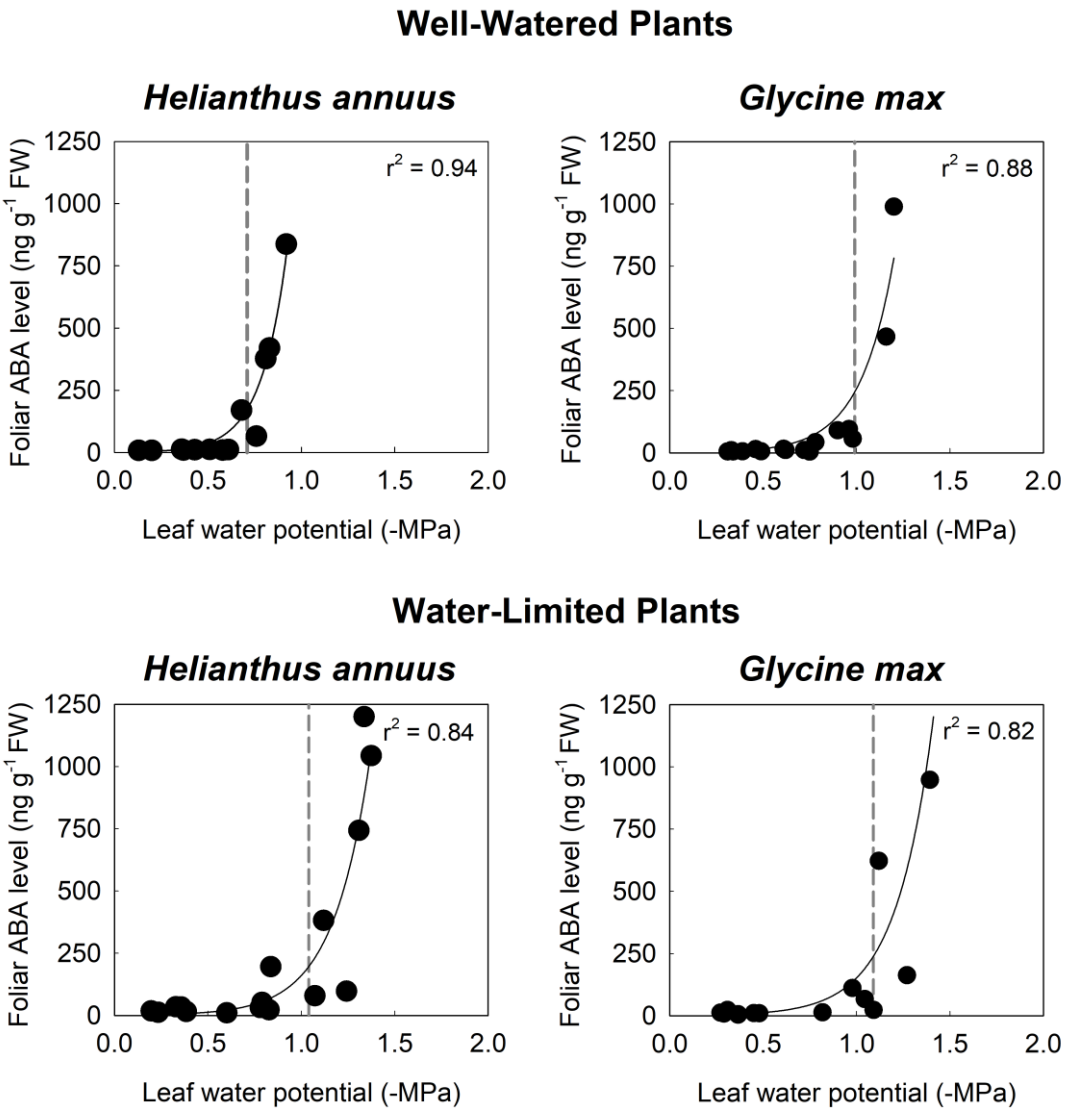
Well-Watered Plants
Helianthus annuus
Glycine max
Foliar ABA level (ng g-1 FW)
Leaf water potential (-MPa)
r2 = 0.94
r2 = 0.88
Water-Limited Plants
r2 = 0.84
r2 = 0.82
0
250
500
750
1000
1250
0.0
0.5
1.0
1.5
2.0

Supplemental Materials

Osmotic adjustment reinforces the key role played by ABA in stomatal responses to vapor pressure deficit in two herbs. Amanda A. Cardoso[1,2], Timothy J. Brodribb[1,*], Fábio M. DaMatta[2], Scott A. M. McAdam[1]

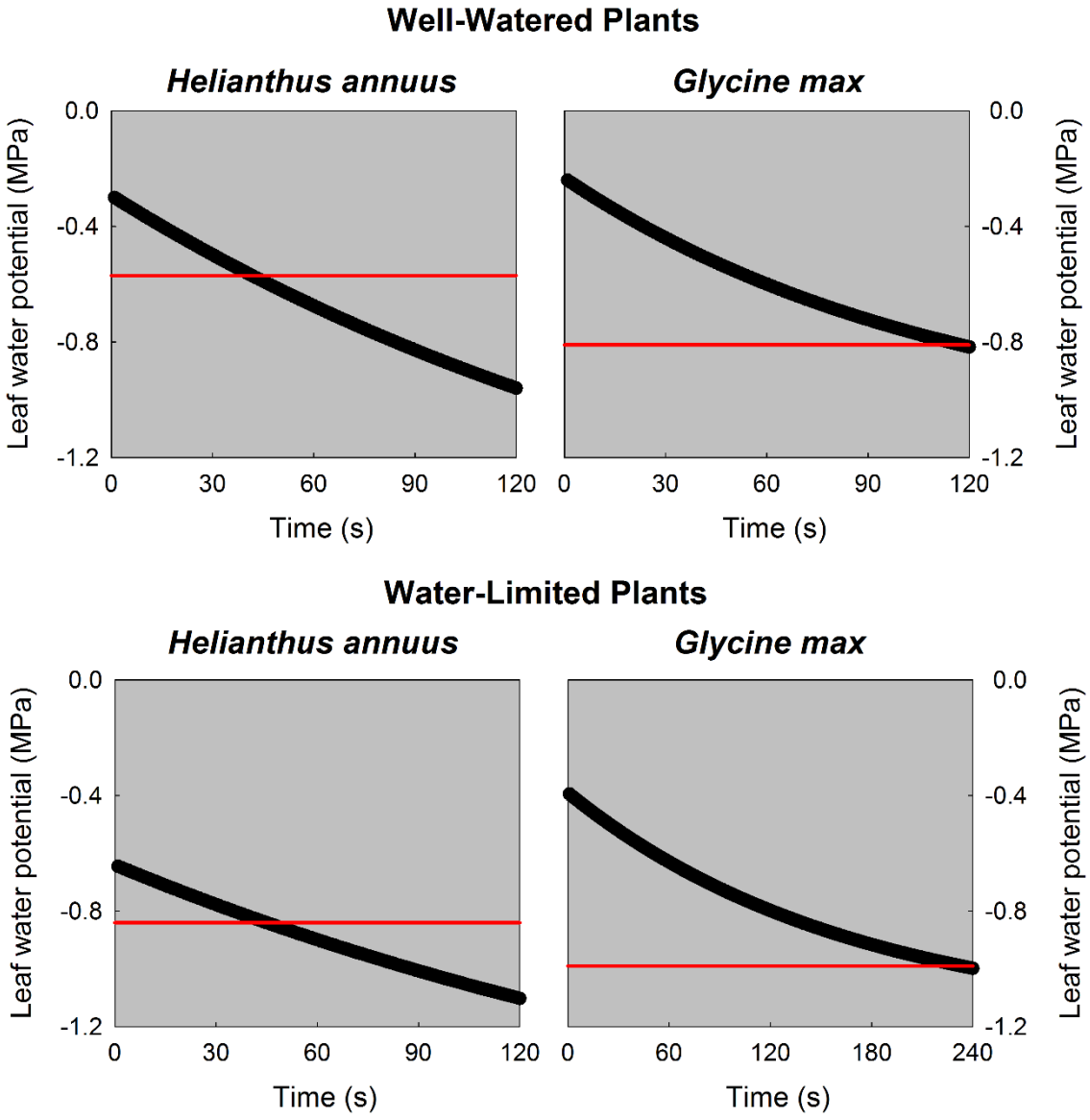

Fig. S1. Modelled dynamic drops in leaf water potential during 120 s or 240 s after VPD transition from 0.5 kPa to 3.0 kPa in well-watered plants and from 1.0 kPa to 3.5 kPa in water-limited plants (see Fig. 3, 4). Model assumed leaf dehydration equivalent to the discharging of a capacitor through a resistor and no stomatal closure during this time. Solid red lines indicate the minimum leaf water potential necessary to trigger the foliar ABA level

accumulated under high VPD, calculated using the relationship between foliar ABA level and leaf water potential (see Fig. 2). VPD, vapor pressure deficit.

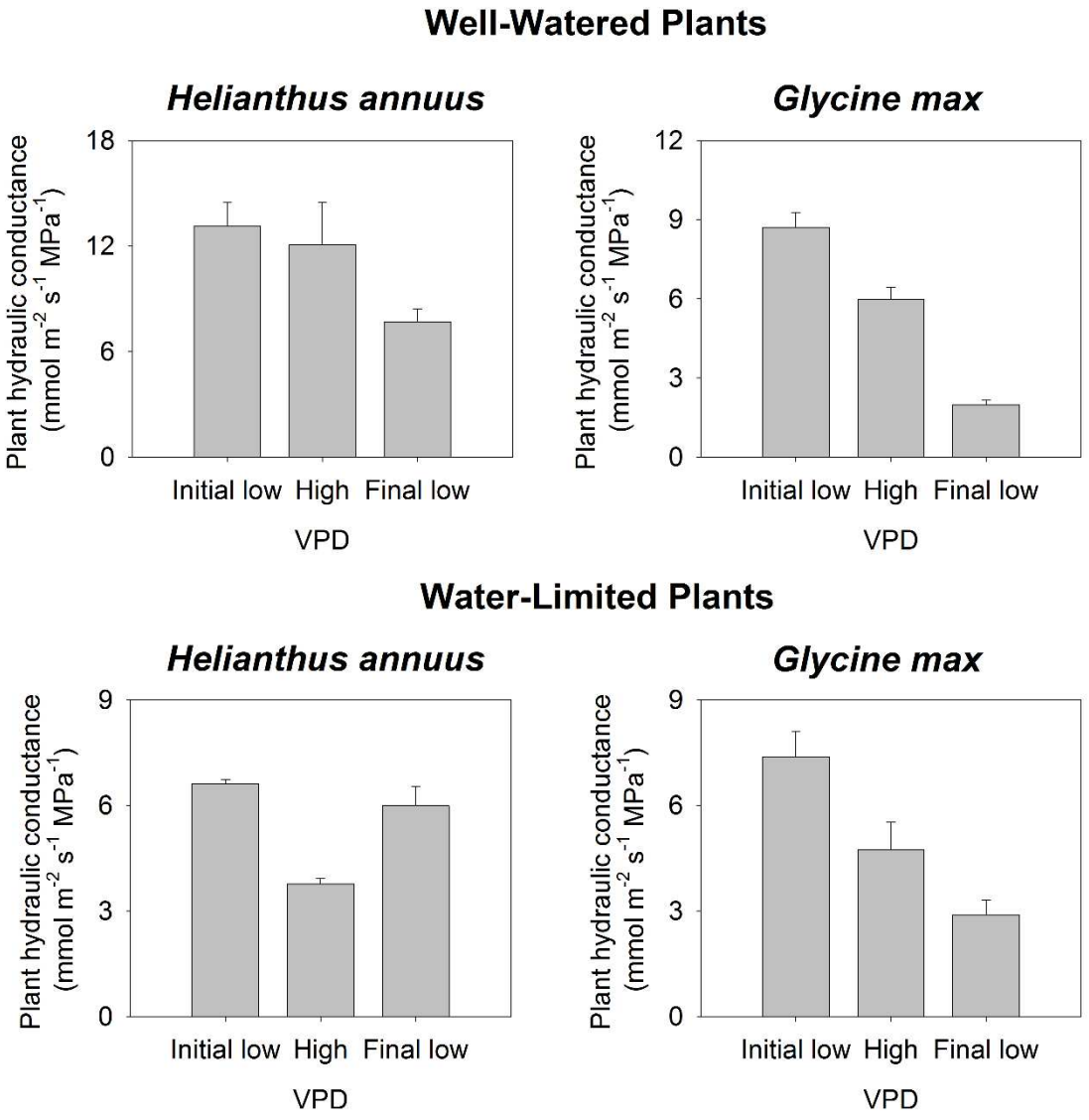

Fig. S2. Mean response of apparent plant hydraulic conductance (n = 3, ± SE) in plants of Helianthus annuus and Glycine max grown under either well-watered or water-limited conditions during reversible sequence of VPD transitions (see Fig. 3, 4). VPD, vapor pressure deficit.

CHAPTER 2

Coordinated plasticity maintains safety in sunflower leaves

Coordinated plasticity maintains safety in sunflower leaves

Amanda A. Cardoso[1,2], Timothy J. Brodribb[1*], Christopher J. Lucani[1], Fábio M. DaMatta[2] and Scott A. M. McAdam[3]

[1]School of Biological Sciences, University of Tasmania, Hobart, TAS 7005, Australia

[2]Departamento de Biologia Vegetal, Universidade Federal de Viçosa, 36570-900 Viçosa, MG, Brazil

[3]Botany and Plant Pathology, Purdue University, West Lafayette, Indiana 47906, USA.

*Corresponding author:

Timothy J. Brodribb

School of Biological Sciences, Private Bag 55, University of Tasmania, Hobart, TAS, 7001, Australia.

Phone: +61 362261707

Email: timothyb@utas.edu.au

ABSTRACT

The air-seeding threshold water potential establishes a hydraulic limit on the ability of woody species to survive in water-limiting environments, but herbs may be more plastic in terms of their ability to adapt to drying conditions. Here we examined the capacity of sunflower (Helianthus annuus L.) leaves to adapt to reduced water availability by modifying the sensitivity of xylem and stomata to soil water deficit. We found that sunflower plants grown under water-limited conditions significantly adjusted leaf osmotic potential, which was linked to a prolongation of stomatal opening as soil dried and a reduced sensitivity of photosynthesis to water-stress induced damage. At the same time, the vulnerability of midrib xylem to cavitation was observed to be highly responsive to growth conditions, with water-limited plants producing conduits with thicker cell walls which were much more resistant to cavitation. Coordinated plasticity in osmotic potential and xylem vulnerability enabled water-limited sunflowers to safely extract water from the soil, while protecting leaf xylem against embolism. High plasticity in sunflower xylem contrasts with data from woody plants, and may suggest an alternative strategy in herbs.

Key-words: cavitation; herbaceous species; osmotic adjustment; stomatal movement; xylem refilling; xylem vulnerability.

INTRODUCTION

Plant water transport through xylem cells is mostly driven by tension gradients generated at air-water interfaces within leaves (Dixon & Joly 1895). Transporting water under tension is free of metabolic costs, however, the instability of water at high tension results in an inevitable consequence: a vulnerability of the xylem to cavitation (Sperry & Tyree 1988). When plants are exposed to drying soils or high evaporative demands, tensions generated in the xylem vasculature can exceed a limit (i.e. 'air-seeding' threshold) where an air bubble is pulled into the conduit lumen, where it rapidly expands to block the conduit to water flow (i.e. embolism; Tyree & Sperry 1989). Drought-induced embolism reduces the plant hydraulic conductance, including leaf hydraulic conductance (K_{leaf}; Brodribb et al. 2016), negatively impacting photosynthetic gas exchange (Sack & Holbrook 2006; Brodribb et al. 2007). The xylem vulnerability to cavitation emerges therefore as a primary constraint on vascular plant-function (Tyree & Sperry 1989).

Xylem vulnerability in herbs has been traditionally difficult to measure due to technical limitations (Lens et al. 2016), but the available data suggest that herbs are highly sensitive to cavitation (Stiller & Sperry 2002; Li et al. 2009; Saha et al. 2009). Recent studies showed that the entire xylem system of tomato plants, including roots, stems and leaves, experienced c. 40% of embolism at the very mild water potential of c. –1.5 MPa (Skelton et al. 2017). Given the tendency for high xylem vulnerability to be associated with low construction cost and high transport efficiency (Hacke et al. 2006; Larter et al. 2015), the expression of vulnerable xylem in herbs certainly accords with the general impression of herbaceousness as occupying the "fast" end of the plant economics spectrum (Reich 2014). Yet at the same time, high vulnerability to cavitation poses questions about the functionality of herbs during water stress. Two scenarios threaten to cause cavitation and loss of productivity in vulnerable herbaceous plants; the first is the possibility of cavitation caused by strong evaporation in well-watered plants, and the second is cavitation produced by soil drying. Many herbs have very high maximum stomatal conductances (g_s), potentially exposing them to massive rates of transpiration, which could drive leaf water potentials (Ψ_{leaf}) sufficiently low to induce cavitation (Oren et al. 1999; Sperry 2000). Stomatal closure in response to declining Ψ_{leaf} has been observed to arrest leaf dehydration before cavitation

(Cochard et al. 2002; Brodribb & McAdam 2017; Martin-StPau et al. 2017) but the possibility of wrong-way stomatal responses (Buckley 2005) caused by very rapid changes in evaporation could allow transient water potential excursions into the danger zone for cavitation. However, the danger of cavitation induced by excessive evaporation in wet soil, may not be especially problematic for herbaceous plants because xylem should refill either by capillarity or by root pressure if plants are allowed to equilibrate with wet soil overnight (Gleason et al. 2017).

Xylem cavitation caused by drying soil poses a potentially more significant threat to xylem-vulnerable herbs because embolisms are unlikely to be repairable until soils return to full hydration and atmospheric humidity approaches 100%. Thus, herbs with highly vulnerable xylem appear to be precariously exposed to changes in soil water content that could cause damage or death. Even if stomatal closure delays the dehydration of the plant body, species with highly vulnerable xylem are incapable of extracting water from drying soil, without risking xylem failure (Choat et al. 2012). This means stomata in water-limited herbs are forced to remain closed, and plants are unable to take up CO_2 for photosynthesis. These potential costs must be balanced by the likely benefits of producing vulnerable xylem such as reduced construction costs or improved efficiency. Quantifying these risks and benefits is essential in order to understand the ecology of herbaceousness.

Here we focus on the risk component associated with constructing highly vulnerable xylem. Of particular interest for herbaceous species living very close to the cavitation limits of their xylem, is whether the potential exists for plastic modification of xylem vulnerability under conditions of water limitation. It is known that herbaceous species are often highly plastic in terms of leaf osmotic adjustment under water limitation, which extends the water potential range of stomatal opening (Turner & Jones 1980). However, such adjustment would appear to expose the xylem to heightened risk of cavitation unless xylem vulnerability could also be shifted to accommodate lower water potentials. Such plasticity could greatly extend the tolerance of otherwise sensitive plants to more negative soil water potentials. The possibility of xylem acclimation during exposure to reduced water availability has been identified as a potentially important issue in woody plants (Anderegg 2014), yet there is little information about plasticity in herbs, where the threat of cavitation is likely to be most

profound. Sunflower (Helianthus annuus L.) makes an ideal subject for examining the impact of water stress on hydraulic vulnerability because this species is known to exhibit plasticity in stomatal response to water potential and leaf turgor in response to changes in growth conditions (Tardieu et al. 1996).

In order to understand whether sunflower plants are able to modify their hydraulic system to accommodate drier growth conditions we measured the xylem vulnerability and stomatal responsiveness to leaf-air vapor pressure deficit (VPD) of plants grown under both well-watered and water-limited soil. We hypothesised that sunflower plants grown under water-limited soils would exhibit leaf xylem that was less vulnerable to embolism, and leaves less vulnerable to photosynthetic damage. We further hypothesised that a coordinated shift of osmotic potential and xylem vulnerability in water-limited plants would play a critical role in prolonging leaf gas exchange while preventing leaf xylem cavitation and declines in whole plant hydraulic conductance (K_{plant}) under high VPD.

MATERIALS AND METHODS

Plant material and growth conditions

Seeds of sunflower cv. Yellow Empress (Asteraceae) were germinated in c. 3 L plastic pots containing potting mix, and watered daily to full capacity until seedlings were c. three weeks old. The plants were next grown under either well-watered or water-limited conditions for another five weeks. Well-watered plants were watered daily to full capacity [predawn water potential ($\Psi_{predawn}$) > –0.30 MPa] (Table 1), and kept in glasshouse regulated at 16-h day at 25°C/15°C day/night temperatures, VPD at c. 1.0 kPa during the day, and natural light [maximum photosynthetic photon flux density (PPFD) of approximately 1500 μmol m^{-2} s^{-1}]. Water-limited plants were watered three times per week to full capacity (–0.50 MPa > $\Psi_{predawn}$ > –1.36 MPa; Table 1), resulting in a clear wilting-recovery cycle (Fig. 1) They were kept outside the glasshouse during summer (from December 2016 to January 2017) under a natural c. 16-h day at c. 23°C/13°C day/night temperatures, VPD at 1.45 ± 0.7 kPa during the day, and natural light (maximum PPFD of approximately 1800 μmol m^{-2} s^{-1}). At the end of the total eight weeks, both well-watered and watered-limited plants were c. 100–120 cm tall, and each plant had c. 20 leaves.

Physiological and anatomical traits

All measurements were carried out using fully expanded leaves developed entirely during the watering treatment period. Leaves from three individuals per treatment were sampled for each measurement.

Predawn and midday Ψ_{leaf} were determined for water-limited plants over the course of the week during the watering treatment period. The midday Ψ_{leaf} was determined as a proxy of minimum Ψ_{leaf} (Ψ_{min}). Leaves were sampled before sunrise (0600 h) and at c. 1200 h., wrapped in damp paper towel, bagged, and immediately measured using a Scholander pressure chamber (615D, PMS Instrument Company, Albany, USA). The $\Psi_{predawn}$ for well-watered plants was measured using a similar approach.

Measurements of the osmotic potential at full turgor (Ψ_s) were carried out using a stem psychrometer (PSY1, ICT International, Armidale, Australia) in a similar way to Bartlett et al. (2012). Leaf discs c. 5 mm in diameter were collected from fully expanded leaves in the early morning after watering (when leaves were close to full hydration). Midribs and large veins were avoided. Tissues were wrapped in aluminium foil, immediately frozen in liquid nitrogen for at least c. 30 min to disrupt cell walls, and sealed stem psychrometers. The Ψ_s was logged every 10 min until stable (c. 30 min).

A second sample of leaves was used to determine the leaf turgor loss point (Ψ_{tlp}) and leaf capacitance (C_{leaf}) using pressure-volume analysis (PV curve; Tyree & Hammel 1972). Fully expanded leaves for each growth condition were cut under water and rehydrated with petioles submerged overnight until Ψ_{leaf} was > –0.1 MPa. Leaf weight and Ψ_{leaf} were measured over time during slow desiccation on the bench until Ψ_{leaf} became difficult to measure due to cell damage. Relative water content was plotted against Ψ_{leaf}^{-1} as per Tyree & Hammel (1972) using the "Pressure volume curve analysis" spreadsheet from Sack et al. (2011). The Ψ_{tlp} was determined by the inflection point between the pre-turgor loss and post-turgor loss portions of the curve, and the C_{leaf} was calculated in terms of relative water content from the linear slope of the plot, and normalized by leaf area.

Fully expanded and visibly undamaged leaves were collected from the third to fifth node from the distal end of the stem. For paradermal analysis, fresh leaves were divided

vertically into two equal parts, and three sections of c. 100 mm^2 (i.e. near the leaf base, in the central region and near the tip) were taken along one of the sides. The sections were cleared using commercial bleach, rinsed, stained with 1% toluidine blue and mounted on microscope slides in phenol glycerine jelly. Three field of view (FOV) per section were photographed using a camera (Digital Sight DS-L1, Nikon, Melville, USA) mounted on a microscope (DM 1000, Leica, Nussloch, Germany), and the images were used to quantify vein density (D_v) and stomatal density (D_s) using the ImageJ software (National Institute of Health, New York, USA). The D_v was measured in one FOV per section at ×4 magnification (FOV area 3.47 mm^2), and D_s was measured in one FOV per section at ×20 magnification (FOV area 0.14 mm^2) on both sides of the leaves. For cross sections, fresh leaves were cut at approximately one-third position from the top to the bottom using a freeze-microtome (BFS-3MP, Physitemp Instruments, Clifton, USA). The sections were stained with 1% toluidine blue, and mounted in phenol glycerine jelly. Three FOVs per section were photographed, and the images were used to quantify leaf thickness (T_{leaf}), hydraulically weighted vessel diameter (D_h) and the xylem cell wall thickness (t) and lumen breadth (b) ratio [$(t/b)^3$; a theoretical predictor of vulnerability to cell collapse; Brodribb & Holbrook 2005]. The T_{leaf} was measured in two FOVs per section at ×10 magnification, and D_h, t and b were measured in one FOV per section at ×40 magnification. Both t and b were measured for all xylem conduits in the midrib; for each conduit b was calculated as the average of the maximum and minimum diameters of each lumen and t was calculated as the average of three random measurements of cell wall thickness. The D_h was calculated for each leaf using the equation:

$$D_h = \sum b^5 / \sum b^4 \text{ (Kolb \& Sperry 1999) (Eqn 1)}$$

The cell wall thickness values used for $(t/b)^3$ calculation was obtained as the value consistent with the D_h using the linear relationship between t and b for each leaf (Blackman et al. 2010).

Optical vulnerability (OV) technique and leaf injury monitoring

Prior to measurement, plants were fully hydrated overnight. In the morning, plants were carefully removed from pots to enhance the rate of soil drying, and one leaf was placed under a stereomicroscope (M205A, Leica Microsystems, Heerbrugg, Switzerland) to record the development of cavitation in the leaf midrib. Water potential was measured at 20 min intervals using a psychrometer attached to the stem and confirmed with twice-daily water

potential measurements using a Scholander pressure chamber. Images of the midrib were taken every 3 min using a camera mounted on the microscope. Images were analysed by quantifying differences in light transmission through the midrib between captured images using an image subtraction method in ImageJ [for details see Brodribb et al. (2016) and www.opensourceov.org]. To analyse the relationship between plant water status and embolism formation, a linear regression was fitted between the time and water potential measurements, and used to determine the water potential at the time of each image capture. These values were then plotted against total embolism area for each image to produce an OV curve. The water potentials at 12%, 50% and 88% of maximum cavitation in the leaf midrib (P_{12}, P_{50} and P_{88}) were calculated based on this vulnerability curve. Each vulnerability curve was measured during c. 72 h, and for all individuals the last midrib cavitation occurred at c. 48 h maximum. The final 24 h were used to ensure no more cavitation events, and to finish collecting fluorescence data. An additional experiment was performed measuring K_{leaf} from well-watered and water-limited plants to confirm that water-limited plants were capable of refilling during the night, confirming that there was minimal embolism present in water-limited leaves prior to the beginning of OV measurements (for further details see the "maximum leaf hydraulic conductance" section).

The maximum quantum efficiency of photosystem II (F_v/F_m) is a well-known parameter typically used as an index of photosynthetic potential and injury in leaves (Guadagno et al. 2017). Here, we assessed F_v/F_m in the same plants used for the OV method over the desiccation course as a proxy for leaf damage. Leaf samples were taken randomly c. four times per day, dark-adapted for 30 min, and F_v/F_m was assessed using a portable chlorophyll fluorometer (PAM-2000, Heinz Walz, Effeltrich, Germany). Leaf tissues were illuminated with weak modulated measuring beams to obtain the initial fluorescence (F_0) and then a saturating white light pulse was applied to ensure maximum fluorescence emissions (F_m), from which F_v/F_m was calculated:

$$F_v/F_m = [(F_m - F_0)/F_m)] \text{ (Eqn 2)}$$

The dynamic changes in F_v/F_m were then presented in response to Ψ_{leaf}.

Vapor pressure deficit transitions

Individual plants were watered and acclimated overnight in a custom-built chamber under dark and low VPD conditions [c. 0.75 kPa (30°C and 82% relative humidity)]. The following day, lights were turned on (300 µmol m^{-2} s^{-1} at the leaf surface), and temperature and VPD maintained at the conditions described above. After stable leaf gas exchange and Ψ_{leaf} were measured under this low VPD condition. Plants were then transferred to an adjacent chamber under a high VPD condition [c. 3.25 kPa (30°C and 23% relative humidity), and the same parameters were measured for a period of 60 min. Plants were ultimately transferred back to the low VPD condition, and the parameters were measured for another 60-min period. Relative humidity was controlled by a condensing dehumidifier (SeccoUltra 00563, Olimpia-Splendid, Gualtieri, Italy). Temperature and relative humidity were monitored every 30 s during the entire experimental period using a humidity probe (HMP45AC, Vaisala, Helsinki, Finland) and a temperature thermocouple; both connected to a data logger (CR800, Campbell Scientific, Logan, USA).

One fully expanded leaf per plant was selected for instantaneous g_s measurements, which were performed using a portable photosynthesis system (GFS-3000, Heinz Walz, Effeltrich, Germany). Conditions in the cuvette were controlled at temperature of 30°C, 390 µmol CO_2 mol^{-1} air, PPFD of 1000 µmol m^{-2} s^{-1} at the leaf surface and the VPD was maintained as close as possible to the ambient chamber VPD. Maximum transient transpiration rate (E) was calculated using g_s (obtained from the gas exchange measurements) and VPD (obtained from the relative humidity of the chamber and leaf temperature measured with a thermocouple). One leaf per plant was sampled for Ψ_{leaf} at each measurement time. After harvesting, leaves were wrapped in wet paper towel, bagged and placed in a humid box for Ψ_{leaf} assessment using a Scholander pressure chamber. Steady-state K_{plant} was further calculated under initial low VPD, high VPD (60 min after the VPD transitions), and on returning to low VPD (60 min after the VPD transitions). Calculation of K_{plant} to the target leaf was made using the equation:

$$K_{plant} = E / \Psi_{leaf} \text{ (Eqn 3)}$$

under steady-state at both low and high VPD, assuming soil water potential in watered pots were close to zero, as all plants, including the water-limited ones, were watered in the night before the experiment.

So as to understand the dynamics of Ψ_{leaf} during a rapid VPD transition, E, g_s, and Ψ_{leaf} were modelled during VPD transitions under the theoretical condition of no stomatal closure and constant g_s. E was calculated using maximum g_s and values of VPD, and a dynamic drop in Ψ_{leaf} was modeled assuming leaf dehydration equivalent to the discharging of a capacitor through a resistor (Brodribb & Holbrook 2003):

$$\Psi_{leaf,\, i+1} = \Psi_{leaf,i} - [\Psi_m - (\Psi_m \times e^{\frac{-t \times K_{plant}}{C_{leaf}}})] \quad \text{(Eqn 4)}$$

where $\Psi_{leaf,i}$ (MPa) is the steady-state Ψ_{leaf} under low VPD; Ψ_m (MPa) is the minimum Ψ_{leaf} that would be reached at steady-state conditions under high VPD, considering the maximum E (E_{max}; mmol m^{-2} s^{-1}; driven by the initial g_s and high VPD) and K_{leaf} (mmol m^{-2} s^{-1} MPa^{-1}), calculated as $\Psi_m = E_{max}/K_{leaf}$; t is the time interval (s); and C_{leaf} unit was mmol m^{-2} MPa^{-1}.

Maximum leaf hydraulic conductance

K_{leaf} was determined in plants grown under well-watered and water-limited conditions. Leaves were sampled from 800 h to 1000 h, after plants had been well watered early in the morning. In addition, three further individuals grown under water-limited conditions were sampled after being watered and bagged for two days in the dark. K_{leaf} was assessed by the evaporative flux method (Sack et al. 2002; Brodribb & Holbrook 2006) using a flowmeter. All individuals were watered and transferred to the laboratory during the morning. The leaves were acclimated to high humidity (bagged with wet paper) for approximately 30 min to ensure high g_s. Leaves were then cut under water and immediately connected to the flowmeter. PPFD of c. 600 μmol m^{-2} s^{-1} and a constant stream of warm air were applied to the leaves (leaf temperature ranged from 27 to 32°C) allowing high rates of transpiration, and consequent high rates of flow. After flow reached a maximum steady-state for c. 5 min, Ψ_{leaf} was immediately measured using a Scholander pressure chamber. Calculation of K_{leaf} was made using the equation:

$$K_{leaf} = F / \Psi_{leaf} \quad \text{(Eqn 5)}$$

where F is the water flow into the leaf at steady-state condition. Values were normalized to leaf area and the viscosity of water at 20°C (Korson et al. 1969). The K_{leaf} were considered maximum in plants grown under well-watered conditions and in plants grown under water-

limited conditions after bagging (i.e. condition under which plants repair xylem embolism due positive root pressure).

Statistical Analysis

Student's t tests (n = 3) were performed to test differences between well-watered and water-limited plants regarding the parameters Ψ_{tlp}, Ψ_s, P_{50}, K_{leaf}, C_{leaf}, D_v, D_s, T_{leaf}, D_h, and $(t/b)^3$. Further Student's t tests (n = 3) were used to compare K_{plant} under low and high VPD within plants from each growth treatment (well-watered or water-limited). In addition, Student's t tests (n = 3) were performed to test differences between water-limited plants either without bagging or after bagging and well-watered plants in terms of K_{leaf}.

RESULTS

Leaf Vulnerability to Embolism and Injury

The $\Psi_{predwan}$ of well-watered plants were higher than c. –0.30 MPa during the entire experimental period, while $\Psi_{predwan}$ of water-limited plants ranged from –0.50 to –1.36 MPa between watering events (Table 1; Fig. 1). Such water shortage during growth induced osmotic adjustments, as evidenced by significant changes in Ψ_s and Ψ_{tlp} in water-limited plants to a lower Ψ_{leaf} compared with well-watered plants (Table 1).

Cavitation was clearly visualized in the sunflower midrib (Fig. 2) with large numbers of events accumulating in a sigmoidal fashion as plants dried. The resultant midrib vulnerability curves were very different for plants grown under the two watering treatments (Fig. 3). Plants grown under water-limited conditions displayed a significantly higher resistance to embolism (P_{50} = –1.74 MPa) than their well-watered counterparts (P_{50} = –1.15 MPa; Table 1; Fig. 3a). A similar pattern was observed regarding P_{12} and P_{88}, i.e. –1.42 and –2.05 MPa for water-limited plants, respectively; and –1.06 and –1.24 MPa for well-watered plants, respectively. The steep slope of the vulnerability curves meant that there was no overlap in the vulnerability curves produced by leaves from the different treatments

Strong coordination between the shift in osmotic potential and xylem vulnerability was evident in terms of a significant correlation between P_{50} and Ψ_s ($r = 0.96$; $P < 0.05$; Fig. 4). In association with changes in P_{50} and Ψ_s in water limited plants, the water potential

threshold triggering a decline in maximum quantum yield of photosystem II (F_v/F_m) also shifted to a more negative water potential in water-limited plants (F_v/F_m < 0.75 at –2.23 ± 0.06 MPa) than well-watered plants (F_v/F_m < 0.75 at –1.63 ± 0.17 MPa; Fig. 3b).

Increases in resistance to embolism in plants grown under water-limited conditions were accompanied by a higher $(t/b)^3$ ratio, driven by significantly differences in the cell wall thickness rather than decreases in D_h (Table 1). Other morpho-physiological traits related to hydraulic efficiency [e.g. maximum K_{leaf}, D_v, D_s, T_{leaf} and D_h] were not significantly different in plants grown under both conditions (Table 1).

VPD Responses of Stomata

When sunflower plants grown under well-watered conditions were transferred from low to high VPD conditions, Ψ_{leaf} fell to values close to the Ψ_{tlp} (Fig. 5b; Table 1) within the first 5 min. This decline was driven by a dramatic initial increase in the transpiration rate (E; considering no stomatal closure immediately after the VPD transition; Fig. 5a). Afterwards, g_s was shown to gradually decrease (Fig. 5c), resulting in a final diminished E (Fig. 5a) and increased Ψ_{leaf} (Fig. 5b). Modeled data indicated that without stomatal closure under high VPD, pronounced declines in Ψ_{leaf} driven by exceedingly high rates of E would lead embolism in the leaf midrib over a very short timeframe (Fig. 5b). No significant difference in apparent K_{plant} measured under steady-state at low and high VPD was observed (Fig. 5d).

When sunflower plants grown under water-limited conditions were exposed to high VPD, similar dynamic changes in E, Ψ_{leaf} and g_s were observed. However, a faster stomatal closure took place in plants grown under water-limited conditions (compare g_s 10 min after the VPD transitions in Figures 5 and 6), likely due to a narrower difference between initial Ψ_{leaf} and Ψ_{tlp} (0.4 MPa in water-limited plants against 0.3 MPa in well-watered plants). This resulted in a considerably lower peak of E than in plants grown under water-limited conditions (compare Figures 5 and 6). A 40% loss of apparent K_{plant} was observed under high VPD compared with low VPD (Fig. 6d), yet Ψ_{leaf} did not fall below the threshold causing incipient embolism (compare Ψ_{leaf} in Figures 6b and 3a). A complete recovery of K_{plant} was observed 60 min after returning to low VPD (K_{plant} = 6.0 ± 0.5 mmol m^{-2} s^{-1} MPa^{-1}).

Repair of Leaf Xylem Embolism

To test whether embolized vessels can be repaired in sunflower plants, we compared K_{leaf} measured in plants grown under water-limited conditions before and after plants had been bagged and darkened for 48 h to maximize the potential for refilling by root pressure with K_{leaf} measured in plants grown under well-watered conditions. We observed that K_{leaf} in plants grown under water-limited conditions were 50% lower compared with plants grown under well-watered conditions (Fig. 7) even after watering. Importantly, however, we found that this reduction in K_{leaf} in water-limited plants could be reversed if plants were re-watered and leaves were bagged (in situ) overnight to ensure 100% humidity (Fig. 7). Considering the Ψ_{min} water-limited plants were exposed to (c. –1.95 MPa; Fig. 1), it would be expected a c. 55% decline in maximum K_{leaf} based on the OV curve (Fig. 3a). This value is consistent with the K_{leaf} measured in water-limited plants non-bagged, as it represents a drop of 45% in K_{leaf} compared with maximum K_{leaf} measured after bagging.

DISCUSSION

Coupling physiological and anatomical data with results from the recently developed OV method (Brodribb et al. 2016), we demonstrate tight coordination between osmotic adjustment in sunflower plants, induced by soil water-stress, and changes in xylem vulnerability to cavitation. The result of parallel adjustment in these key physiological traits is that water-limited sunflowers were able to extract more water from soils without risking xylem cavitation or leaf damage. Further, stomatal responsiveness to VPD was found to efficiently prevent xylem embolism in sunflowers exposed to dry atmospheres under either wet or dry soils. Adjustments in xylem vulnerability in response to dry soils, stomatal closure in response to dry atmospheres, and osmotic adjustment to protect photosynthetic systems are proposed as crucial mechanisms allowing survival of sunflower plants under water-limited conditions.

Coordinated plasticity in hydraulic and stomatal dynamics enables safer water extraction from drier soils

Sunflower leaves are known to substantially adjust osmotic potential (Ψ_s) when exposed to dry soil (Turner et al. 1978). This was clearly confirmed here. Adjustment of cellular solute potential in water-limited plants provided leaves with the advantage of sustaining gas exchange and photosynthesis as $\Psi_{predawn}$ dropped. Our principle question was

to determine how a species that was vulnerable to xylem cavitation could freely adjust Ψ_s, reducing stomatal and photosynthetic sensitivity to water potential, without incurring costs in terms of xylem dysfunction caused by cavitation as Ψ_{leaf} dropped during the day. The answer to this question was revealed in terms of a remarkable degree of plasticity in xylem vulnerability of sunflower leaves. As a result, we found coordinated changes in solute potential, stomatal and photosystem sensitivity to water potential, and xylem vulnerability. This coordinated response enabled sunflower to respond to drier soil by enhancing water extraction capacity while maintaining xylem safety by stomatal closure.

The resistance to xylem cavitation is recognized as a key trait limiting species ability to survive during soil drought (Choat et al. 2012; Skelton et al. 2017), in addition to determining species distribution (Blackman et al. 2012; Larter et al. 2017). Furthermore, as the threshold water potential for air-seeding is thought to exhibit low plasticity in plant species (Choat et al. 2012; Lamy et al. 2014), it is tempting to expect that highly vulnerable species, such as sunflower, would be restricted to wet environments. Contrary to this hypothesis, sunflower plants are commonly found to survive under relatively dry conditions (e.g. Tardieu et al. 1996). Our results provide an explanation for these observations, by demonstrating high plasticity in xylem vulnerability in sunflower that enables plants grown under water-limited conditions to maintain the integrity of their water transport system under conditions that would be lethally damaging in unadjusted plants (Figs. 3 and 4). These results contrast with previous studies reporting very low levels of within-species variation in P_{50} of stems (Corcuera et al. 2011; Plavcová et al. 2011) and leaves (Nolf et al. 2016; Blackman et al. 2017). Given that leaves have a shorter lifespan, and greater exposure to variation in water potential than stems, it seems likely that leaves may exhibit a higher degree of plasticity in vulnerability than stems. When considered in the context of low relatively low plasticity of stem vulnerability in sunflower (Stiller & Sperry 2002; Delzon in press), this seems to be the case for this species. Additionally, it is notable that sunflower appears to exhibit a higher degree of vulnerability segmentation than other herbs such as tomato (Skelton et al. 2017). The ecology of segmentation among herbs and woody plants seems to be quite diverse, and will be a rich field for future research.

Less vulnerable xylem is expected to attract costs in terms of xylem construction, as the development of more negative pressures within the conduits could result in cell collapse if leaf xylem were not sufficiently reinforced to withstand mechanical rupture (Hacke et al. 2001; Blackman et al. 2010). In this regard, our results demonstrate that reductions in xylem vulnerability in osmotically adjusted plants were also accompanied by thicker cell wall in the xylem conduits of the midrib, and hence higher $(t/b)^3$ (Table 1). This more mechanically reinforced xylem could resist more negative xylem pressures before buckling and becoming non-conductive during water stress (Zhang et al. 2016).

As well as producing more robust xylem, we found that the photosynthetic apparatus was more robust to dehydration in water-limited plants. Based upon declines in F_v/F_m, we provide compelling evidence that complete hydraulic failure in the midrib precedes drought damage in terms of leaf injury in sunflower (Fig. 3), much like previous studies that associate leaf damage with extensive embolism, i.e. starting from P_{88} to P_{95} (Brodribb & Cochard 2009; Skelton et al. 2017).

As sunflower leaves dehydrate, a conservative sequence of physiological events occurs: loss of turgor, xylem embolism and ultimately tissue injury (Fig. 3). Similar patterns have been previously discussed (Brodribb et al. 2003; Nolf et al. 2016; Maréchaux et al. 2017) and here we provide further insights on (i) how such sequence is functionally important to prevent drought-induced xylem embolism and consequent major losses of hydraulic conductance, and on (ii) physiological mechanisms in angiosperms that enable plasticity in stomatal closure to avoid drought-induced damage, (iii) and most importantly, how changing the threshold for one of these physiological mechanisms in sunflower results in a parallel shift in all mechanisms.

Stomatal closure is usually associated with turgor loss, and in angiosperm species is driven by a non-hydraulic signal, i.e. ABA. Bulk Ψ_{tlp} has long been recognized to induce major augmentation of foliar ABA levels during acute drought (Pierce & Raschke 1980), as well as changes in turgor prior to complete turgor loss has been very recently proposed to stimulate subtle yet functional levels of foliar ABA during VPD transitions (McAdam & Brodribb 2016). In this regard, our VPD data (Figs. 5 and 6) demonstrate that as soon as VPD increases, Ψ_{leaf} transiently decreases breaching Ψ_{tlp} within minutes (compare Ψ_{tlp} and Ψ_{leaf} at

5 min in high VPD; Figs. 5 and 6), and consequently inducing stomatal closure very likely due to ABA signalling. Such fast and efficient stomatal closure prevents further decreases in Ψ_{leaf}, which could otherwise result in xylem embolism. Without stomatal closure under high VPD (dotted lines in Figures 5b and 6b), 88% xylem embolism in the leaf midrib would occur in less than 10 min after a switch from low to high VPD in sunflower plants (Figs. 5 and 6). This result per se strongly pinpoints stomatal closure as an exceedingly important mechanism by which herbs prevent hydraulic failure under high VPD, adding to the well-known importance of stomatal closure to prevent cavitation during soil water stress in woody plants (Brodribb et al. 2017; Martin-StPau et al. 2017). We further suggest that the higher water potential for leaf turgor loss compared with xylem embolism is an important prerequisite for stomatal closure preventing embolism during VPD transitions, and the greater the distance between Ψ_{tlp} and P_{50}, the safer for the plant.

By protecting xylem against embolism, plants avoid significant losses of xylem hydraulic conductance (Brodribb et al. 2016). However, variations in outside-xylem hydraulic conductances, e.g. leaf or cell shrinkage, as well as deactivation of membrane aquaporins outside the xylem, have been also reported to reduce hydraulic conductances (Scoffoni et al. 2017). While recovery in xylem hydraulic conductance depends on xylem refilling (McCully et al. 1998; Gleason et al. 2017), declines in outside-xylem hydraulic conductance (K_{ox}) appear to be rapidly reversed after watering (Zhang et al. 2016; Scoffoni et al. 2017). In this regard, it is possible that declines in K_{ox} either in leaves or roots may have contributed to reductions in K_{plant} in sunflower plants grown under water-limited conditions when exposed to high VPD (Fig. 6d), given that depressed K_{plant} recovered to initial levels 60 min after returning to low VPD. However, the depression of K_{plant} at high VPD was not seen in well watered plants, undermining support for variable K_{ox} as a general driver of VPD responses in sunflower. We reiterate turgor loss and consequent foliar ABA increases, as the primary cause of stomatal closure under high VPD, as inferred from the pronounced stomatal closure despite any changes in the steady-state K_{plant} in well-watered plants (Fig. 5d). In any case, it is possible that reductions in K_{plant} under high VPD in water-limited plants may have also contributed to further stomatal closure (Scoffoni et al. 2017).

Embolism refilling emerges as an ultimate mechanism to maintain leaf hydraulic conductance in herbaceous plants

Our results suggest that declines in K_{leaf} in water-limited plants resulted from cavitation events, and this could be reversed when plants were well watered and bagged overnight, likely due to positive root pressure (Fig. 7). If declines in K_{leaf} were driven by reduced outside-xylem hydraulic conductance (Zhang et al. 2016), this decline would be reversed immediately upon watering. However, this was not the case, and K_{leaf} recovered completely only when plants were watered and bagged for two successive nights. In addition, the percentage drop in K_{leaf} measured in water-limited plants is consistent with the percentage of cumulative embolism as expected from the vulnerability curves (Fig. 3a).

ACKNOWLEDGEMENTS

The authors gratefully acknowledge funding support from the Australian Research Council [grants nos. DE140100946 (S.A.M.M.) and DP140100666 (T.J.B.)] and the Brazilian agency FAPEMIG [grant no. BDS-00404-15 (A.A.C.)]. CSIRO Hobart is also acknowledged for stem psychrometers used during the experiments.

REFERENCES

Anderegg W.R.L. (2014) Spatial and temporal variation in plant hydraulic traits and their relevance for climate change impacts on vegetation. New Phytologist **205**, 1008–1014.

Bartlett M.K., Scoffoni C., Ardy R., Zhang Y., Sun S., Cao K. & Sack L. (2012) Rapid determination of comparative drought tolerance traits: using an osmometer to predict turgor loss point. Methods in Ecology and Evolution **3**, 880–888.

Blackman C.J., Aspinwall M.J., Tissue D.T. & Rymer P.D. (2017) Genetic adaptation and phenotypic plasticity contribute to greater leaf hydraulic tolerance in response to drought in warmer climates. Tree Physiology **37**, 583–592.

Blackman C.J., Brodribb T.J. & Jordan G.J. (2010) Leaf hydraulic vulnerability is related to conduit dimensions and drought resistance across a diverse range of woody angiosperms. New Phytologist **188**, 1113–1123.

Blackman C.J., Brodribb T.J. & Jordan G.J. (2012) Leaf hydraulic vulnerability influences species' bioclimatic limits in a diverse group of woody angiosperms. Oecologia **168**, 1–10.

Brodribb T.J. & Cochard H. (2009) Hydraulic failure defines the recovery and point of death in water-stressed conifers. Plant Physiology **149**, 575–584.

Brodribb T.J., Feild T.S. & Jordan G.J. (2007) Leaf maximum photosynthetic rate and venation are linked by hydraulics. Plant Physiology **144**, 1890–1898.

Brodribb T.J. & Holbrook N.M. (2003) Stomatal closure during leaf dehydration, correlation with other leaf physiological traits. Plant Physiology **132**, 2166–2173.

Brodribb T.J. & Holbrook N.M. (2005) Water stress deforms tracheids peripheral to the leaf vein of a tropical conifer. Plant Physiology **137**, 1139–1146.

Brodribb T.J. & Holbrook N.M. (2006) Declining hydraulic efficiency as transpiring leaves desiccate: two types of response. Plant, Cell *&* Environment **29**, 2205–2215.

Brodribb T.J., Holbrook N.M., Edwards E.J. & Gutiérrez M.V. (2003) Relations between stomatal closure, leaf turgor and xylem vulnerability in eight tropical dry forest trees. Plant, Cell *&* Environment **23**, 443–450.

Brodribb T.J. & McAdam S.A.M. (2017) Evolution of the stomatal regulation of plant water content. Plant Physiology **174**, 639–649.

Brodribb T.J., McAdam S.A.M. & Murphy M.R.C. (2017) Xylem and stomata, coordinated through time and space. Plant, Cell & Environment **40**, 872–880.

Brodribb T.J., Skelton R.P., McAdam S.A.M., Bienaimé D., Lucani C.J. & Marmottant P. (2016) Visual quantification of embolism reveals leaf vulnerability to hydraulic failure. New Phytologist **209**, 1403–1409.

Buckley T.N. (2005) The control of stomata by water balance. New Phytologist **168**, 275–292.

Choat B., Jansen S., Brodribb T.J., Cochard H., Delzon S., Bhaskar R., …, Zanne A.E. (2012) Global convergence in the vulnerability of forests to drought. Nature **7426**, 752–755.

Cochard H., Coll L., Le Roux X. & Améglio T (2002) Unraveling the effects of plant hydraulics on stomatal closure during water stress in walnut. Plant Physiology **128**, 282–290.

Corcuera L., Cochard H., Gil-Pelegrin E. & Notivol E. (2011) Phenotypic plasticity in mesic populations of Pinus pinaster improves resistance to xylem embolism (P_{50}) under severe drought. Trees **25**, 1033–1042.

Dixon H.H. & Joly J. (1895) The path of the transpiration current. Annals of Botany **9**, 416–419.

Gleason S.M., Wiggans D.R., Bliss C.A., Young J.S., Cooper M., Willi K.R. & Comas L.H. (2017) Embolized stems recover overnight in Zea mays: the role of soil water, root pressure, and nighttime transpiration. Frontiers in Plant Science **8**, 1–11.

Guadagno C.R., Ewers B.E., Speckman H.N., Aston T.L., Huhn B.J., DeVore S.B., …, Weinig C. (2017) Dead or alive? Using membrane failure and chlorophyll a fluorescence to predict plant mortality from drought. Plant Physiology pp.00581.2016

Hacke U.G., Sperry J.S., Pockman W.T., Davis S.D. & McCulloch K.A. (2001) Trends in wood density and structure are linked to the prevention of xylem implosion by negative pressure. Oecologia **126**, 457–461.

Hacke U.G., Sperry J.S., Wheeler J.K. & Castro L. (2006) Scaling of angiosperm xylem structure with safety and efficiency. Tree Physiology **26**, 689–701.

Kolb K.J. & Sperry J.S. (1999) Differences in drought adaptation between subspecies of Sagebrush (Artemisia tridentata). Ecology **80**, 2373–2384.

Korson L., Drost-Hansen W. & Millero F.J. (1969) Viscosity of water at various temperatures. The Journal of Physical Chemistry A **73**, 34–39.

Lamy J-B., Delzon S., Bouche P.S., Alia R., Vendramin G.G., Cochard H. & Plomion C. (2014) Limited genetic variability and phenotypic plasticity detected for cavitation resistance in a Mediterranean pine. New Phytologist **201**, 874–886.

Larter M., Brodribb T., Pfautsch S., Burlett R., Cochard H. & Delzon S. (2015) Extreme aridity pushes trees to their physical limits. Plant Physiologist **168**, 804–807.

Larter M., Pfautsch S., Domec J.C., Trueba S., Nagalingum N. & Delzon S. (2017) Aridity drove the evolution of extreme embolism resistance and the radiation of conifer genus Callitris. New Phytologist **215**, 97–112.

Lens F., Picon-Cochard C., Delmas C.E., Signarbieux C., Buttler A., Cochard H., …, Delzon S. (2016) Herbaceous angiosperms are not more vulnerable to drought-induced embolism than angiosperm trees. Plant Physiology **172**, 661–667.

Li Y., Sperry J.S. & Shao M. (2009) Hydraulic conductance and vulnerability to cavitation in corn (Zea mays L.) hybrids of differing drought resistance. Environmental and Experimental Botany **66**, 341–346.

Maréchaux I., Bartlett M.K., Iribar A., Sack L. & Chave J. (2017) Stronger seasonal adjustment in leaf turgor loss point in lianas than trees in an Amazonian forest. Biology Letters 13: 20160819.

Martin-StPaul N., Delzon S. & Cochard H. (2017) Plant resistance to drought depends on timely stomatal closure. Ecology Letters doi: 10.1111/ele.12851.

McAdam S.A.M. & Brodribb T.J. (2016) Linking turgor with ABA biosynthesis: implications for stomatal responses to vapor pressure deficit across land plants. Plant Physiology **171**, 2008–2016.

McCully M., Huang C. & Ling L. (1998) Daily embolism and refilling of xylem vessels in the roots of field-grown maize. New Phytologist **138**, 327–342.

Nolf M., Rosani A., Ganthaler A., Beikircher B. & Mayr S. (2016) Herb hydraulics: inter- and intraspecific variation in three Ranunculus species. Plant Physiology **170**, 2085–2094.

Oren R., Sperry J.S., Katul G., Pataki D.E., Ewers B.E., Phillips N. & Schafer K.V.R. (1999) Survey and synthesis of intra- and inter specific variation in stomatal sensitivity to vapor pressure deficit. Plant, Cell *&* Environment **22**, 1515–1526.

Pierce M. & Raschke K. (1980) Correlation between loss of turgor and accumulation of abscisic acid in detached leaves. Planta **148**, 174–182.

Plavcová L., Hacke U.G. & Sperry J.S. (2011) Linking irradiance-induced changes in pit membrane ultrastructure with xylem vulnerability to cavitation. Plant, Cell & Environment **34**, 501–513.

Reich P.B. (2014) The world-wide 'fast–slow' plant economics spectrum: A traits manifesto. Journal of Ecology **102**, 275–301.

Sack L. & Holbrook N.M. (2006) Leaf hydraulics. Annual Review of Plant Biology **57**, 361–381.

Sack L., Melcher P.J., Zwieniecki M.A. & Holbrook N.M. (2002) The hydraulic conductance of the angiosperm leaf lamina: a comparison of three measurement methods. Journal of Experimental Botany **53**, 2177–2184.

Sack L., Pasquet-Kok J. & PrometheusWiki contributors (2011) Leaf pressure-volume curve parameters. URL http://prometheuswiki.publish.csiro.au/tiki-index.php?page=Leaf+pressure-volume+curve+parameters. [accessed 10 March 2017].

Saha S., Holbrook N.M., Montti L., Goldstein G. & Cardinot G.K. (2009) Water relations of Chusquea ramosissima and Merostachys claussenii in Iguazu national park, Argentina. Plant Physiology **149**, 1992–1999.

Scoffoni C., Albuquerque C., Brodersen C., Townes S.V., John G.P., …, Sack L. (2017) Outside-xylem vulnerability, not xylem embolism, controls leaf hydraulic decline during dehydration. Plant Physiology **173**, 1197–1210.

Skelton R.P., Brodribb T.J. & Choat B. (2017) Casting light on xylem vulnerability in an herbaceous species reveals a lack of segmentation. New Phytologist **214**, 561–569.

Sperry J.S. (2000) Hydraulic constraints on gas exchange. Agricultural and Forest Meteorology **104**, 13–23.

Sperry J.S. & Tyree M.T. (1988) Mechanism of water stress induced xylem embolism. Plant Physiology **88**, 581–587.

Stiller V. & Sperry J.S. (2002) Cavitation fatigue and its reversal in sunflower (Helianthus annuus L.). Journal of Experimental Botany **53**, 1155–1161.

Tardieu F., Lafarge T. & Simonneau T.H. (1996) Stomatal control by fed or endogenous xylem ABA in sunflower: interpretation of correlations between leaf water potential and stomatal conductance in anisohydric species. Plant, Cell *&* Environment **19**, 75–84.

Turner N.C., Begg J.E. & Tonnet M.L. (1978) Osmotic adjustment of sorghum and sunflower crops in response to water deficits and its influence on the water potential at which stomata close. Functional Plant Biology **5**, 597–608.

Turner N.C. & Jones H.G. (1980) Turgor maintenance by osmotic adjustment: a review and evaluation. In Adaptation of Plants to Water and High Temperature Stress (eds Turner N.C. & Kramer P.J.), pp. 87–103. Wiley Interscience, New York.

Tyree M.T. & Hammel H.T. (1972) The measurement of the turgor pressure and the water relations of plants by the pressure-bomb technique. Journal of Experimental Botany **23**, 267–282.

Tyree M.T. & Sperry J.S. (1989) Vulnerability of xylem to cavitation and embolism. Annual Review of Plant Physiology and Plant Molecular Biology **40**, 19–38.

Zhang Y.J., Rockwell F.E., Graham A.C., Alexander T. & Holbrook N.M. (2016) Reversible leaf xylem collapse: a potential "circuit breaker" against cavitation. Plant Physiology **172**, 2261–2274.

TABLES

Table 1. Mean values (n = 3, ± SE) for predawn water potential ($\Psi_{predawn}$; MPa), water potential at turgor loss point (Ψ_{tlp}; -MPa), osmotic potential at full turgor (Ψ_s; -MPa), water potential at 50% cumulative embolism (P_{50}; -MPa), maximum leaf hydraulic conductance (K_{leaf}; mmol m^{-2} s^{-1} MPa^{-1}), leaf capacitance (C_{leaf}; mmol m^{-2} MPa^{-1}), vein density (D_v; mm mm^{-2}), stomatal density (D_s; mm^{-2}) on the lower epidermis, leaf thickness (T_{leaf}; mm), hydraulically weighted vessel diameter ($D_{h;}$ x 10^2), and xylem cell wall thickness (t; mm) and lumen breadth (b; mm) ratio $(t/b)^3 \, x \, 10^3$] in Helianthus annuus plants grown under either well-watered or water-limited conditions.

Traits	Well-watered	Water-limited
$\Psi_{predawn}$	> –0.30	–0.50 to –1.36
Ψ_{tlp}	0.71 ± 0.03	$1.04 \pm 0.02^{**}$
Ψ_s	0.50 ± 0.01	$0.95 \pm 0.05^{*}$
P_{50}	1.15 ± 0.07	$1.74 \pm 0.04^{**}$
K_{leaf}	11.88 ± 1.14	11.05 ± 0.16^{ns}
$C_{leaf,}$	3064 ± 102	3417 ± 211^{ns}
D_v	11.31 ± 0.54	11.58 ± 0.17^{ns}
D_s	286 ± 15	320 ± 30^{ns}
T_{leaf}	0.233 ± 0.01	0.254 ± 0.01^{ns}
D_h	2.32 ± 0.17	2.18 ± 0.08^{ns}
$(t/b)^3$	1.10 ± 0.29	$4.03 \pm 0.33^{**}$

Asterisks indicate significant changes in each trait (Student's t test; *, $P < 0.05$; **, $P < 0.01$; ns not significant) between growth conditions.

FIGURE LEGENDS

Figure 1. Mean predawn water potential ($\Psi_{predawn}$; black circles) and minimum leaf water potential (Ψ_{min}; white circles) over the course of the week observed in Helianthus annuus plants (n = 3, ± SD) grown under water-limited conditions. Short-dashed black lines indicate when plants were watered.

Figure 2. A spatio-temporal map showing the progression of embolisms events in the leaf midrib recorded in Helianthus annuus plants grown under well-watered conditions during the desiccation. The colour scale shows the leaf water potential (Ψ_{leaf}; MPa) at which different cavitation events occurred. Time ranges after excision are shown in each panel.

Figure 3. (a) Comparison of the percentage cumulative total embolism in the leaf midrib recorded during drying between Helianthus annuus plants grown under both well-watered (grey symbols) and water-limited (black symbols) conditions. The different symbols indicate individual leaves. The dashed vertical lines show the mean turgor loss points for plants grown under either well-watered (grey lines) or water-limited (black lines) conditions. (b) Comparison of maximum quantum yield (F_v/F_m) recorded during drying between H. annuus plants grown under both well-watered (grey symbols) and water-limited (black symbols) conditions. The different symbols indicate individual leaves. The dashed vertical lines show leaf water potentials at 100% loss of xylem function in the leaf midrib for plants grown under either well-watered (grey lines) or water-limited (black lines) conditions.

Figure 4. Correlation between water potential at 50% cumulative embolism in the leaf midrib (P_{50}) and osmotic potential at full turgor (Ψ_s) in Helianthus annuus plants grown under well-watered (open circles; n = 3) and water-limited condition (filled circles; n = 3). Dashed lines represent turgor loss point (MPa) of plants grown under well-watered (grey line) and water-limited condition (black line).

Figure 5. (a-c) Dynamic response of transpiration rate (E), leaf water potential (Ψ_{leaf}) and stomatal conductance (g_s) in Helianthus annuus plants grown under well-watered conditions exposed to a step change in vapor pressure deficit (VPD) from c. 0.75 kPa (white region) to c. 3.25 kPa (grey region). The different colours indicate individual plants. Dotted lines indicate how these parameters would behave considering no stomatal closure during the VPD

transition. Water potentials at 12%, 50% and 88% cumulative embolism in the leaf midrib (P_{12}, P_{50} and P_{88}) are depicted in (c). (d) Mean apparent plant hydraulic conductance (K_{plant}) in H. annuus plants grown under well-watered conditions (n = 3, ± SE) under steady-state at both 0.75 kPa and 3.25 kPa conditions. Stars denote significant changes (Student's t test; *, $P < 0.05$; **, $P < 0.01$; ns not significant) between VPD conditions.

Figure 6. (a-c) Dynamic response of transpiration rate (E), leaf water potential (Ψ_{leaf}) and stomatal conductance (g_s) in Helianthus annuus plants grown under water-limited conditions exposed to a step change in vapor pressure deficit (VPD) from c. 0.75 kPa (white region) to c. 3.25 kPa (grey region). The different colours indicate individual plants. Dotted lines indicate how these parameters would behave considering no stomatal closure during the VPD transition. Water potentials at 12%, 50% and 88% cumulative embolism in the leaf midrib (P_{12}, P_{50} and P_{88}) are depicted in (c) (d) Mean apparent plant hydraulic conductance (K_{plant}) in H. annuus plants grown under water-limited conditions (n = 3, ± SE) under steady-state at both 0.75 kPa and 3.25 kPa conditions. Stars denote significant changes (Student's t test; *, $P < 0.05$; **, $P < 0.01$; ns not significant) between VPD conditions.

Figure 7. Mean leaf hydraulic conductance (K_{leaf}) in Helianthus annuus plants (n = 3, ± SE) grown under either well-watered or water-limited conditions. Water-limited plants bagged for two days in the dark also had their K_{leaf} assessed. Stars denote significant changes (Student's t test; *, $P < 0.05$; **, $P < 0.01$; ns not significant) between well-watered plants and each other condition.

Figure 1

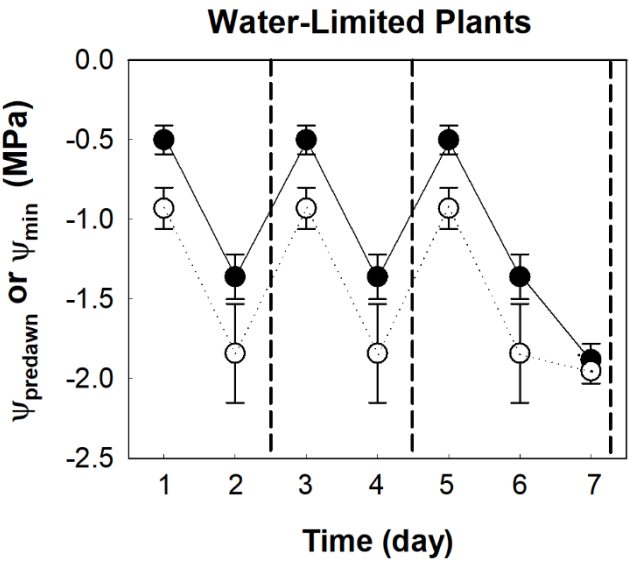
Water-Limited Plants
0.0
-0.5
-1.0
-1.5
-2.0
-2.5
$\psi_{predawn}$ or ψ_{min} (MPa)
1
2
3
4
5
6
7
Time (day)

Figure 2

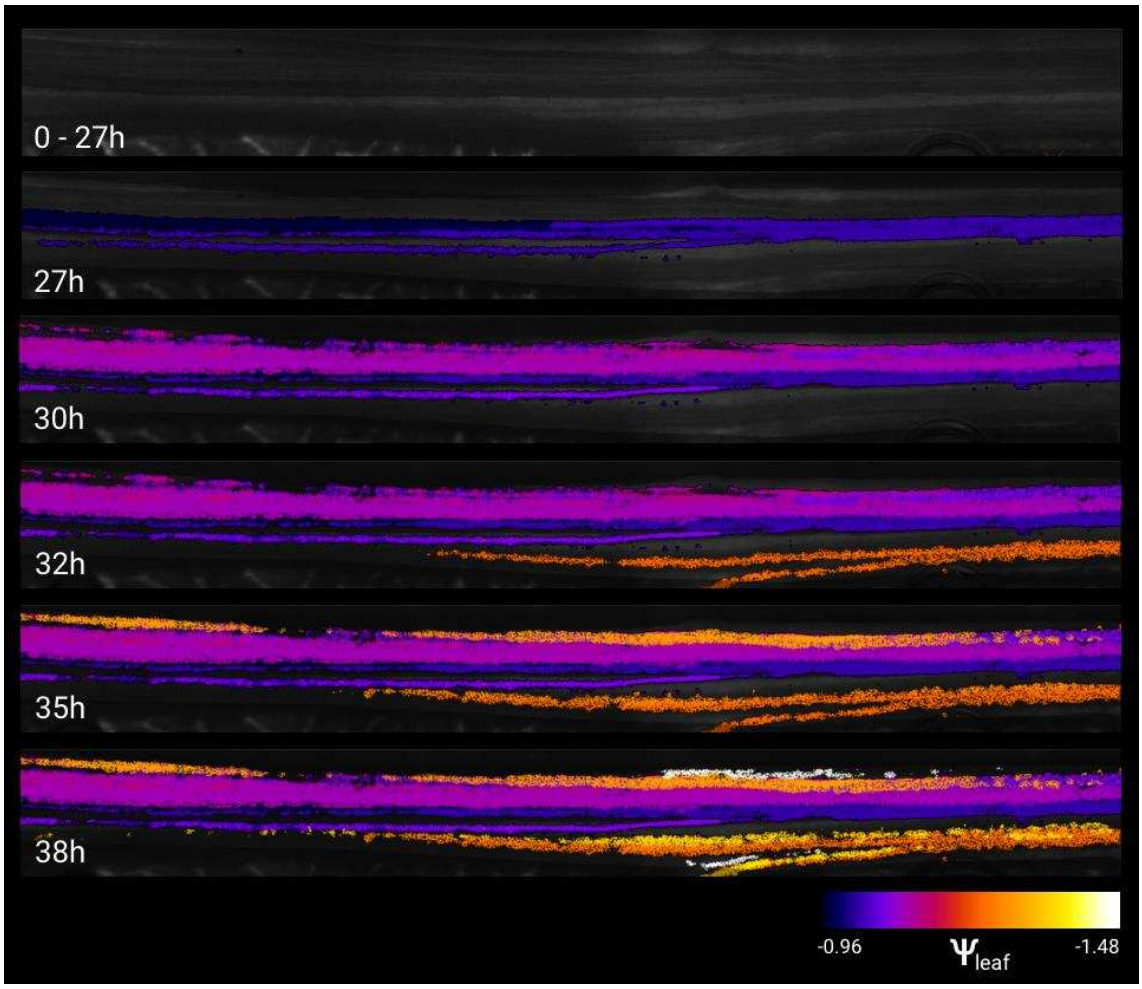

Figure 3

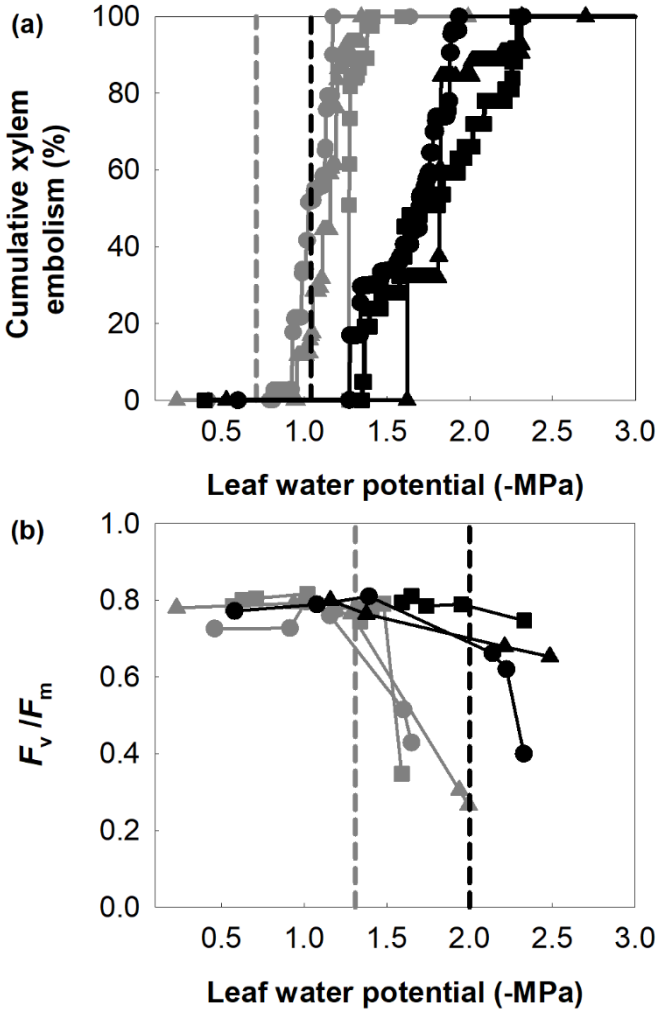
(a)
Cumulative xylem embolism (%)
100
80
60
40
20
0
0.5
1.0
1.5
2.0
2.5
3.0
Leaf water potential (-MPa)
(b)
F_v/F_m
1.0
0.8
0.6
0.4
0.2
0.0
0.5
1.0
1.5
2.0
2.5
3.0
Leaf water potential (-MPa)

Figure 4

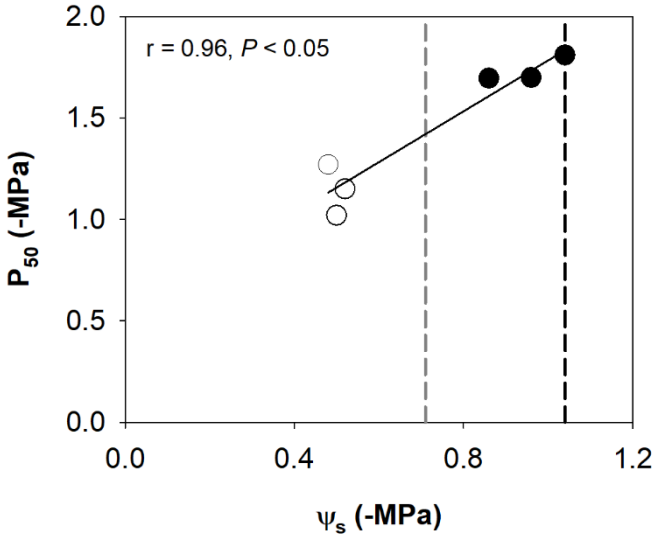

Figure 5

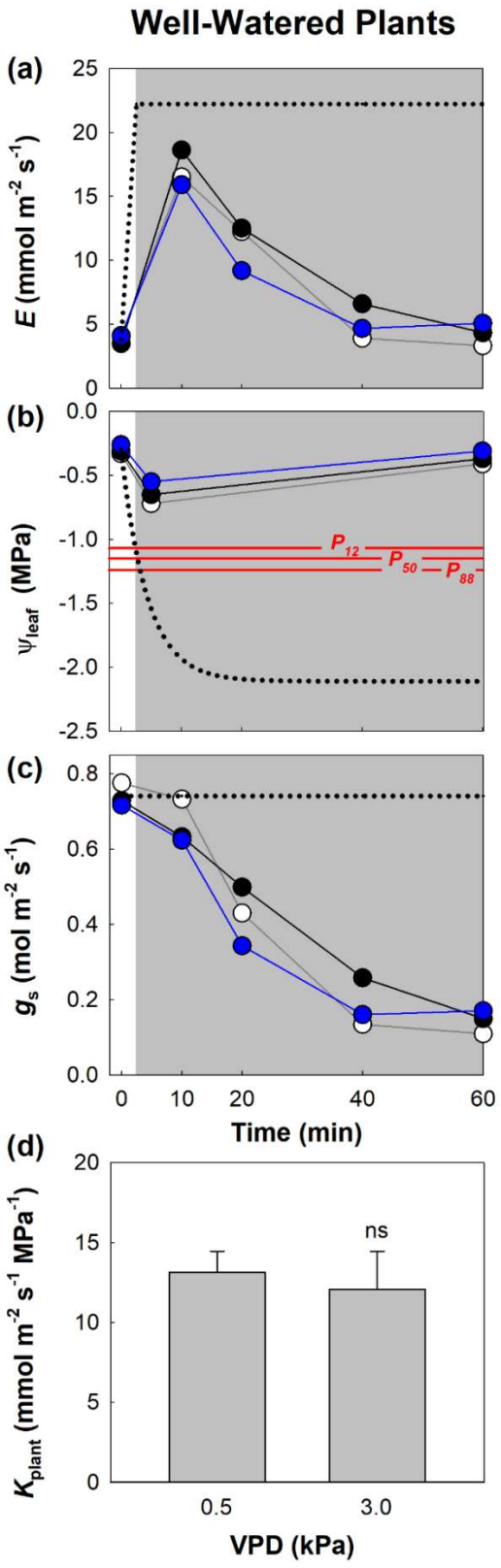
Well-Watered Plants
(a)
E (mmol m-2 s-1)
25
20
15
10
5
0
(b)
ψleaf (MPa)
0.0
-0.5
-1.0
-1.5
-2.0
-2.5
P12
P50
P88
(c)
gs (mol m-2 s-1)
0.8
0.6
0.4
0.2
0.0
0
10
20
40
60
Time (min)
(d)
Kplant (mmol m-2 s-1 MPa-1)
20
15
10
5
0
ns
0.5
3.0
VPD (kPa)

Figure 6

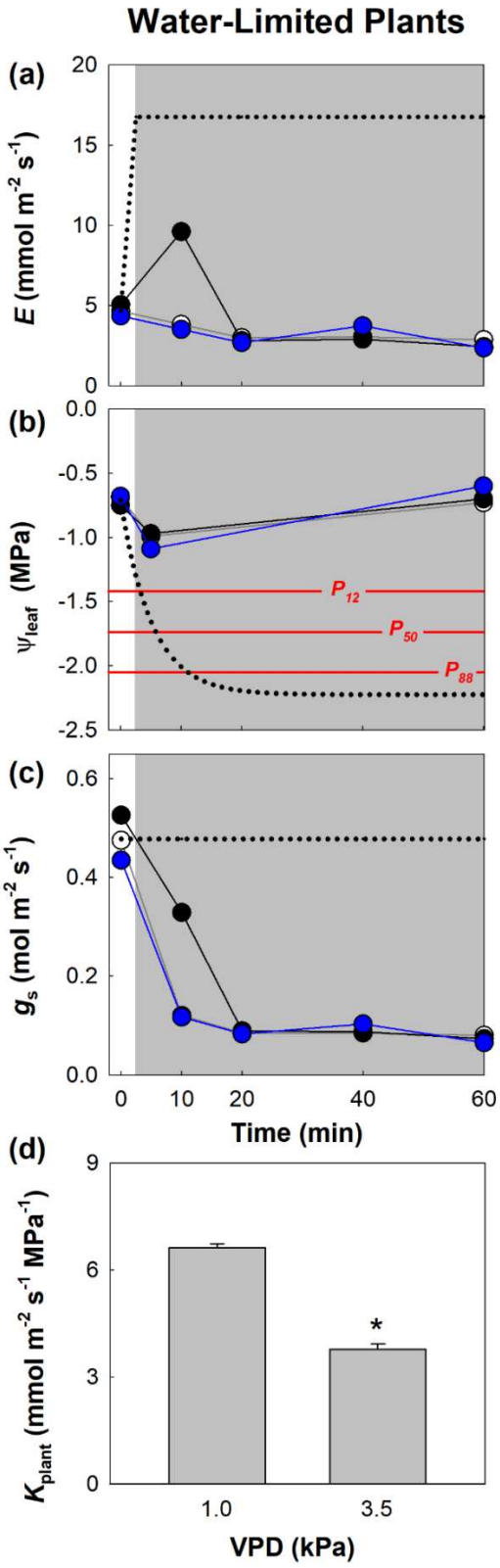
Water-Limited Plants
(a)
E (mmol m-2 s-1)
20
15
10
5
0
(b)
ψleaf (MPa)
0.0
-0.5
-1.0
-1.5
-2.0
-2.5
P12
P50
P88
(c)
gs (mol m-2 s-1)
0.6
0.4
0.2
0.0
0
10
20
40
60
Time (min)
(d)
Kplant (mmol m-2 s-1 MPa-1)
9
6
3
0
*
1.0
3.5
VPD (kPa)

Figure 7

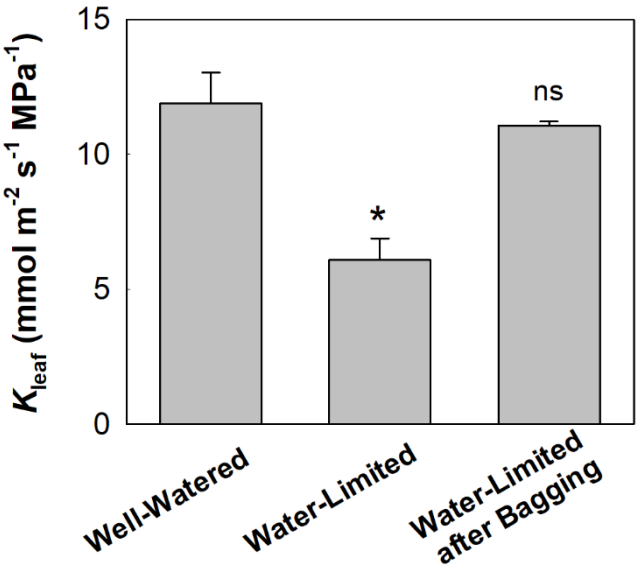
15
10
5
0
K_{leaf} (mmol m^{-2} s^{-1} MPa^{-1})
ns
*
Well-Watered
Water-Limited
Water-Limited after Bagging

GENERAL CONCLUSION

We demonstrate that during leaf-to-air vapor pressure deficit (VPD) transitions, subtle increases in foliar abscisic acid (ABA) levels in two herbs, i.e. sunflower and soybean, are responsible for stomatal closure under high VPD, and the remaining ABA levels for hysteresis in stomatal action on returning to low VPD. Foliar ABA production is likely to be triggered by changes in leaf turgor rather than leaf water potential per se. Whether reductions in leaf turgor or complete turgor loss of some cells within the leaf are responsible for triggering ABA production during VPD transitions remain to be further examined. These results were obtained by examining well-watered and water-limited herbs, which were osmotically adjusted. We observed that these plants were capable of maintaining stomata open under lower leaf water potentials, as it is expected for all osmotically adjusted plants, without showing declines in leaf hydraulic conductance. In further experiments, we observed that a coordinated plasticity in xylem vulnerability to cavitation and stomatal sensitivity to water deficit enabled water-limited sunflowers to safely extract water from the soil, while protecting leaf xylem against embolism. This high plasticity in sunflower xylem vulnerability to cavitation may suggest an alternative strategy in herbaceous species during drought.